The performance of the one-sided truncated exponentially weighted moving average X control chart in the presence of measurement errors

Fupeng Xie, Philippe Castagliola, Anan Tang, Xuelong Hu, Jinsheng Sun

The performance of the one-sided truncated exponentially weighted moving average $\bar{X}$ control chart in the presence of measurement errors

FuPeng Xie [*1], **Philippe Castagliola**[2], **AnAn Tang**[3], **XueLong Hu**[3] **and JinSheng Sun**[4]

[1]*School of Automation, Nanjing Institute of Technology, Nanjing, China*

[2]*Université de Nantes & LS2N UMR CNRS 6004, Nantes, France*

[3]*School of Management, Nanjing University of Posts and Telecommunications, Nanjing, China*

[4]*School of Automation, Nanjing University of Science and Technology, Nanjing, China*

Abstract

When the direction of a potential mean shift can be anticipated, the one-sided exponentially weighted moving average (EWMA) $\bar{X}$ control chart using the truncation method (namely, the one-sided TEWMA $\bar{X}$ chart) is more efficient than those conventional one- and two-sided EWMA $\bar{X}$ schemes for process monitoring. Although attractive, there are no studies on designing the one-sided TEWMA $\bar{X}$ chart by taking measurement errors into account. In this context, we investigate the effect of measurement errors on the performance of the one-sided TEWMA $\bar{X}$ chart based on the linear covariate error model. Additionally, a Markov chain model is established to evaluate the run length properties of the scheme in the presence of measurement errors. Then, an optimal design procedure is developed for searching the optimal design parameters of the scheme. Based on these mentioned studies, several tables and figures are presented to evaluate the detecting performance of the scheme under different parameters of the linear covariate error model, and then

*Corresponding Author: FuPeng Xie. Email: xie_fupeng@163.com

a conventional one-sided EWMA $\bar{X}$ chart with reflecting boundary is introduced to further study the effect of the presence and absence of measurement errors on control chart comparison studies . Simulation results show that although the detecting performance of the proposed scheme is significantly affected by measurement errors, its performance is still superior to the classic competing chart under the same comparison conditions. Finally, an illustrative example is given to show the implementation of the recommended scheme.

Keywords: One-sided EWMA $\bar{X}$ control chart; Measurement errors; Markov chain model; Truncation method; Average run length;

1 Introduction

As one of the most influential tools in statistical process control (SPC), control charts have been extensively used in many fields, for instance, manufacturing industry (see Mukherjee & Marozzi (2021)), service process (see Yang & Jiang (2019)), health surveillance (see García-Bustos & Zambrano (2022)). According to Montgomery (2012), control charts can be classified into two categories: the memoryless-type charts (also named as the Shewhart-type charts) and the memory-type charts. As only the current sample information is considered, Shewhart-type charts are easy to implement and sensitive in detecting large shifts, but this fact also makes it inefficient for monitoring small to moderate shifts in a process. Conversely, by taking both the current and past information into account, memory-type charts (for example, the exponentially weighted moving average (EWMA) and cumulative sum (CUSUM) charts) can be regarded as good alternatives to the memoryless-type charts in monitoring small to moderate shifts. This feature makes memory-type charts to be efficient, and then motivates more meaningful research works, for instance, readers can refer to Hossain et al. (2019), Li et al. (2023) and Perry (2020).

Control charts are usually designed as two-sided type schemes that can monitor both upward and downward shifts in the process. However, in practice, there are many scenarios that only need to focus on one particular shift direction, for instance, the CDC (say, Center for Disease Control) is usually more concerned with the increase in infection rate of a specific disease. As pointed by Chiu

& Tsai (2013), compared with the one-sided type schemes, the conventional two-sided type schemes may spend more time to generate an out-of-control signal when a shift occurs in the process. In this context, it is better to develop and implement a one-sided type control chart, if the direction of the shift can be anticipated or when the investigator is only interested in a particular directional shift. More specifically, two commonly used one-sided EWMA charts are introduced in this paper, one is the one-sided EWMA chart with reflecting boundary (hereafter denoted as the one-sided REWMA chart), and the other is the one-sided EWMA chart using truncation method (hereafter denoted as the one-sided TEWMA chart). Compared with the one-sided TEWMA chart, the one-sided REWMA chart proposed by Gan (1993a) seems more well-studied due to its ease of understanding. According to Shu et al. (2007) and Xie et al. (2022a), the significant difference between these two schemes is the one-sided methodology they used, taking the upward shift monitoring as an example, the charting statistic of the upper-sided REWMA chart is $W_{R,t}^{+} = \max\{B_U, \lambda X_t + (1-\lambda)W_{R,t-1}^{+}\}$, where $\lambda \in (0, 1]$ is the smoothing parameter, and B_U represents the reflecting boundary of the upper-sided REWMA chart. It is not difficult to find that the basic idea of the one-sided REWMA chart is to reset the EWMA charting statistic to the value of the reflecting boundary whenever it is below (or above) the reflecting boundary for the upper-sided (or lower-sided) REWMA chart. Up to now, the reflecting boundary methodology is still widely used in many studies, for instance, Haq (2020) developed the one-sided MEWMA charts with reflecting boundaries for monitoring the mean of a multivariate normal process, and Hu et al. (2023) designed the one-sided EWMA charts using reflecting boundaries for high-quality process monitoring. Obviously, the reflecting boundaries can help to improve the sensitivity of the one-sided REWMA chart, but the difference choices of it can lead to different performance of the scheme. This means that for any specified shift level, if one wants to achieve good detection results, the optimal value of the reflecting boundary needs to be searched before starting the process monitoring. With no doubt, this procedure will complicate the solution. As a suitable alternative, Shu et al. (2007) proposed the one-sided TEWMA chart for monitoring normally distributed data. Similarly, taking upward shift monitoring as an example, the charting statistic of the upper-sided TEWMA chart can be given as $W_{T,t}^{+} = \lambda X_t^{+} + (1-\lambda)W_{T,t-1}^{+}$, where $X_t^{+} = \max(\mu_0, X_t)$, and μ_0 denotes the known in-control mean. As it can be seen, the basic idea of the one-sided TEWMA chart is to accumulate positive (or negative) deviations from the target only, and to truncate negative (or pos-

itive) deviations from the target to zero in the computation of the EWMA statistic at each timestep. Based on this one-sided methodology, Xie et al. (2022a) developed a one-sided adaptive TEWMA chart for detecting both small and large mean shifts simultaneously. Meanwhile, a new one-sided TEWMA TBE chart is recommend by Xie et al. (2022b) to monitor high-quality processes.

Although attractive, all studies mentioned above are based on the assumption that the quality characteristics can be accurately obtained, which seems somewhat unrealistic in practice. In industrial applications, accurate measurement of quality characteristics are often difficult to achieve in situations where humans are involved. According to Noor-ul-Amin & Riaz (2021), measurement error can be defined as the deviation between the gauged value and the actual value of an observation. It always occurs with the same intensity and does not vary from one observation to the next. As summarized by Maleki et al. (2017), the measurement error model can commonly be divided into three categories: (1) the additive model, (2) the multiplicative model, and (3) two- or four-component model. It is worth noting that, Bennett (1954) firstly investigated the effect of measurement errors on the $\bar{X}$ chart using the additive model. On the basis of this research, Linna & Woodall (2001) proposed the most widely used linear covariate model, and then the properties of the Shewhart $\bar{X}$ and the S^2 charts have been investigated in the presence of measurement errors. As one of the main conclusion of this study, using multiple measurements to compensate the negative effect of measurement errors is recommended. Additionally, unlike the constant variance assumption used in linear covariate model, Montgomery & Runger (1993) pointed out that in some circumstances, the variance of the measurement error changes linearly with the process mean level. Hence, researchers have also conducted some works on the model with linearly increasing variance, for instance, readers can refer to Maravelakis (2012) and Khati Dizabadi et al. (2016).

No matter what model is used, the performance of control charts can be more or less affected under the presence of measurement errors. For example, Tran et al. (2021) investigated the effect of measurement errors on the performance of the VSI EWMA median chart, and proved that the measurement errors can significantly affect the detecting performance of the schemes. Tang et al. (2018) studied the performance of the adaptive EWMA $\bar{X}$ chart when the measurement error is defined with

the linear covariate error model, and then the presence of measurement error with a linearly increasing standard deviation has also been investigated. Haq et al. (2015) investigated the effect of measurement errors on the detecting performance of EWMA charts based on various ranked set sampling schemes. By reviewing those related research works, it is not difficult to see that the effect of measurement errors on many two-sided type control charts has been well investigated, but there is little research on one-sided type control charts, especially on the one-sided EWMA type charts. Motivated by the fact that the one-sided methodology (i.e., both the reflecting boundary and the truncation method) can substantially improve the performance of the scheme when the direction of the shift can be anticipated, the goal of this study is to investigate the effect of measurement on the one-sided TEWMA $\bar{X}$ chart, and then compare the performance of the one-sided TEWMA $\bar{X}$ chart with that of the one-sided REWMA $\bar{X}$ chart in the presence of measurement errors. The key contributions of this study can be summarized as following:

- To study the run length (RL) properties of the one-sided TEWMA $\bar{X}$ control chart in the presence of measurement errors.
- To construct the Markov chain model for evaluating the average run length (ARL) of the one-sided TEWMA $\bar{X}$ chart based on the linear covariate error model.
- To compare the ARL performance of the one-sided TEWMA $\bar{X}$ chart with that of the one-sided REWMA $\bar{X}$ chart, in the absence and presence of measurement errors, using the optimal design parameters.

The outline of this study is organized as follows: Firstly, the linear covariate error model is presented in Section 2. Then, in Section 3, the one-sided TEWMA $\bar{X}$ control chart with measurement errors is proposed, and the Markov chain model is established to investigated the ARL performance of the scheme. Furthermore, in the presence of measurement errors, the optimal design procedure of the scheme is developed, and the optimal design parameters are searched. In Section 4, the comparative scheme, say, the one-sided REWMA $\bar{X}$ control chart, is introduced for the comparison with the one-sided TEWMA $\bar{X}$ chart, and some guidelines for using the one-sided TEWMA $\bar{X}$ chart to detect the mean shifts in the presence of measurement errors are also provided. Subsequently, an illustrative example is given in Section 5 to demonstrate the implementation of the one-sided TEWMA $\bar{X}$ chart

with measurement errors. Finally, Section 6 concludes with some remarks and directions for future researches.

2 The linear covariate error model

In this paper, let us assume that the Phase II subgroups $\{X_{t,1}, X_{t,2} \cdots, X_{t,n}\}$ with n independent and identically distributed (iid) normal random variables are available. The true value of the quality characteristic $X_{t,i}$ follows the normal distribution with known in-control mean μ_0 and variance σ_0^2, say, $X_{t,i} \sim N(\mu_0, \sigma_0^2)$, where $i = 1, 2, \cdots, n$. When the process is out-of-control, the process variance keeps unchanged, and the process mean shifts from μ_0 to $\mu = \mu_0 + \delta\sigma_0$, where δ represents the standardized mean shift. As suggested by Linna & Woodall (2001), the true value of the quality characteristic $X_{t,i}$ may not be obtained directly, but it can be assessed from the values $\{Y_{t,i,1}, Y_{t,i,2} \cdots, Y_{t,i,m}\}$ of a set of m measurement operations with each $Y_{t,i,j}$ being equal to

$$Y_{t,i,j} = A + BX_{t,i} + \varepsilon_{t,i,j} \tag{1}$$

where $j = 1, 2, \cdots, m$, A and B denote two known constants, and $\varepsilon_{t,i,j}$ is an independent normal $N(0, \sigma_M^2)$ random error term. According to Tang et al. (2018), to keep the units of μ and σ_M the same, the standard deviation σ_M, instead of the variance σ_M^2, can either be change linearly with the process mean μ (namely, $\sigma_M = C + D\mu$, where C and D are two known extra parameters), or it can be a constant independent of the variable $X_{t,i}$.

In order to compensate for the adverse effect of measurement errors, many researchers suggested to take multiple measurement operations per item in each sample, for instance, see Linna & Woodall (2001), Costa & Castagliola (2011), Nguyen et al. (2020), and the corresponding results have shown that the standard deviation of the measurement error component decreases as the number of measurement operations m increases. At any sampling point $t = 1, 2, \cdots$, when $i = 1, 2, \cdots, n$, and $j = 1, 2, \cdots, m$, $n \times m$ observations $Y_{t,i,j}$ can be easily obtained. Based on these observations, the

sample mean $\bar{Y}_t$ equals to

$$\bar{Y}_t = \frac{1}{nm}\sum_{i=1}^{n}\sum_{j=1}^{m} Y_{t,i,j} = A + \frac{1}{n}\left(B\sum_{i=1}^{n} X_{t,i} + \frac{1}{m}\sum_{i=1}^{n}\sum_{j=1}^{m}\varepsilon_{t,i,j}\right) \tag{2}$$

It is easy to prove that the mean E($\bar{Y}_t$) and the variance V($\bar{Y}_t$) of $\bar{Y}_t$ are equal to

$$E(\bar{Y}_t) = A + B\mu_0 \tag{3}$$

$$V(\bar{Y}_t) = \frac{1}{n}\left(B^2\sigma_0^2 + \frac{\sigma_M^2}{m}\right) \tag{4}$$

respectively.

3 The one-sided TEWMA $\bar{X}$ chart with measurement errors

Let us assume that the quality characteristic X_t needs to be monitored in a process, and $\{X_{t,1}, X_{t,2}, \cdots, X_{t,n}\}$ is a sample of $n > 1$ independent normal random variables taken at regular sampling point $t = 1, 2, \cdots$. For the one-sided TEWMA $\bar{X}$ chart assuming that there is no measurement errors in the quality characteristic X_t, it is appropriate to use the sample mean $\bar{X}_t = \sum_{i=1}^{n} X_{t,i}$ to plot on the scheme for process monitoring.

3.1 The design of the one-sided TEWMA $\bar{X}$ chart

In this section, the upper-sided and lower-sided TEWMA $\bar{X}$ charts using the truncation method are suggested for quickly detecting upward and downward mean shifts, respectively. According to the basic idea of the truncation method, the upper- and lower-truncated variables $\bar{X}_t^+$ and $\bar{X}_t^-$ can be defined as follows:

$$\bar{X}_t^+ = \max(\mu_0, \bar{X}_t) \tag{5}$$

$$\bar{X}_t^- = \min(\mu_0, \bar{X}_t) \tag{6}$$

where μ_0 is the known in-control mean value, and $\bar{X}_t \sim N(\mu_0, \sigma_0^2/n)$. Similarly, in presence of measurement errors, based on Equation (2), the upper- and lower-truncated variables $\bar{Y}_t^+$ and $\bar{Y}_t^-$ can

be given as follows:

$$\bar{Y}_t^+ = \max(\mu_0, \bar{Y}_t) \tag{7}$$

$$\bar{Y}_t^- = \min(\mu_0, \bar{Y}_t) \tag{8}$$

respectively. According to Equation (3), it is easy to know that $\bar{Y}_t \sim N(A + B\mu_0, (B^2\sigma_0^2 + \frac{\sigma_M^2}{m})/n)$, so the upper- and lower-truncated variables with measurement errors can be rewritten as,

$$\bar{S}_t^+ = \max\left(\frac{\mu_0 - E(\bar{Y}_t)}{\sqrt{V(\bar{Y}_t)}}, \bar{S}_t\right) \tag{9}$$

$$\bar{S}_t^- = \min\left(\frac{\mu_0 - E(\bar{Y}_t)}{\sqrt{V(\bar{Y}_t)}}, \bar{S}_t\right) \tag{10}$$

where

$$\bar{S}_t = \frac{\bar{Y}_t - E(\bar{Y}_t)}{\sqrt{V(\bar{Y}_t)}} \sim N(0, 1) \tag{11}$$

In this paper, if we define

$$\frac{\mu_0 - E(\bar{Y}_t)}{\sqrt{V(\bar{Y}_t)}} = \frac{\sqrt{n}(\mu_0 - (A + B\mu_0))}{\sqrt{B^2\sigma_0^2 + \frac{\sigma_M^2}{m}}} = \mu_M \tag{12}$$

Then, the upper- and lower-truncated variables $\bar{S}_t^+$ and $\bar{S}_t^-$ are simply restated as follows:

$$\bar{S}_t^+ = \max\left(\mu_M, \bar{S}_t\right) \tag{13}$$

$$\bar{S}_t^- = \min\left(\mu_M, \bar{S}_t\right) \tag{14}$$

For the monitoring process, if it is deemed to be in-control, the mean and variance of the upper-truncated variable $\bar{S}_t^+$ are

$$E(\bar{S}_t^+) = \mu_M\Phi(\mu_M) + \phi(\mu_M) \tag{15}$$

$$V(\bar{S}_t^+) = 1 - \Phi(\mu_M) + \mu_M\phi(\mu_M) + \mu_M^2\Phi(\mu_M) - (\mu_M\Phi(\mu_M) + \phi(\mu_M))^2 \tag{16}$$

respectively, where $\phi(\cdot)$ and $\Phi(\cdot)$ represent the probability density function (p.d.f.) and the cumulative distribution function (c.d.f.) of the standard normally distributed random variable $\bar{S}_t$ presented in Equation (11). Similarly, the in-control mean and variance values of the lower-truncated variable $\bar{S}_t^-$ are

$$E(\bar{S}_t^-) = \mu_M \left(1 - \Phi(\mu_M)\right) - \phi(\mu_M) \tag{17}$$

$$V(\bar{S}_t^-) = \mu_M^2 \left(1 - \Phi(\mu_M)\right) + \Phi(\mu_M) - \mu_M \phi(\mu_M) - \left(\mu_M - \mu_M \Phi(\mu_M) - \phi(\mu_M)\right)^2 \tag{18}$$

respectively. For more details about the derivation of the mean and variance values of the upper- and lower-truncated variables $\bar{S}_t^+$ and $\bar{S}_t^-$, readers can refer to Appendix A. Furthermore, in this study, the standard form of normal variable $\bar{Z}_t = (\bar{S}_t - E(\bar{S}_t)/\sqrt{V(\bar{S}_t)}$ can be used to simplify the design of the proposed chart. More Specifically, let us define the standard upper- and lower-truncated variables $\bar{Z}_t^+$ and $\bar{Z}_t^-$ as follows:

$$\bar{Z}_t^+ = \frac{\bar{S}_t^+ - E(\bar{S}_t^+)}{\sqrt{V(\bar{S}_t^+)}} \tag{19}$$

$$\bar{Z}_t^- = \frac{\bar{S}_t^- - E(\bar{S}_t^-)}{\sqrt{V(\bar{S}_t^-)}} \tag{20}$$

Based on these two standard upper- and lower-truncated variables, the upper- and lower-sided TEWMA $\bar{X}$ charts can be designed with the following charting statistics:

- For the upward mean shift detection, the charting statistic Q_t^+ of the upper-sided TEWMA $\bar{X}$ chart, at sampling point $t = 1, 2, \cdots$, is defined as:

$$Q_t^+ = \lambda \bar{Z}_t^+ + (1 - \lambda) Q_{t-1}^+ \tag{21}$$

- Meanwhile, for detecting downward mean shifts, the charting statistic Q_t^- of the lower-sided TEWMA $\bar{X}$ chart can be written as:

$$Q_t^- = \lambda \bar{Z}_t^- + (1 - \lambda) Q_{t-1}^- \tag{22}$$

where $\lambda \in (0, 1]$ represents the smoothing parameter of the schemes, and the initial values of $Q_0^+ = Q_0^- = E(Z_t^+) = E(Z_t^-) = 0$. In process monitoring, the upper-sided (or lower-sided) TEWMA $\bar{X}$ chart triggers an out-of-control signal whenever the charting statistic $Q_t^+ > H^+$ ($Q_t^- < H^-$), where H^+ (H^-) is the upper (lower) control limit of the proposed scheme.

3.2 The Markov chain model for the one-sided TEWMA $\bar{X}$ chart

To evaluate the run length (RL) properties of control charts, there are commonly three ways: (1) the Monte Carlo simulation, (2) the Markov chain model, and (3) the integral equations. Among them, the Monte Carlo simulation and the Markov chain model are more widely used and easier to understand. So far, there are many representative and classic studies on these two methods. For example, for Monte Carlo simulation, reader can refer to Schaffer & Kim (2007) and Dickinson et al. (2014). Meanwhile, for Markov chain model, reader can refer to Gan (1993b), Shu & Jiang (2006) and Castagliola et al. (2016). In this study, a Markov chain model is proposed to evaluate the average run length (ARL) performance of the one-sided TEWMA $\bar{X}$ chart with measurement errors. Due to the space limitation, only the upper-sided TEWMA $\bar{X}$ chart with measurement errors is discussed here for illustration.

Without loss of generality, the basic idea of constructing a Markov chain model is to define the transition states by dividing the in-control region into a finite number of subintervals, and then using the midpoint value of each subinterval to approximate the transient state of charting statistic at sampling point. In this paper, the in-control region is divided into M subintervals, and according to Li et al. (2014), the ARL value of the one-sided TEWMA $\bar{X}$ chart can be computed using

$$\mathrm{ARL} = \mathbf{p}^{\mathsf{T}}(\mathbf{I} - \mathbf{Q})^{-1}\mathbf{1}, \tag{23}$$

where $\mathbf{p} = (p_1, p_2, \cdots, p_M)^{\mathsf{T}}$ is the initial probability vector, and $\mathbf{Q}$ is the $M \times M$-dimensional matrix that contains the transition probability elements $q_{i,j}$ of the charting statistic Q_t^+ from state i to state j. Besides, $\mathbf{1}$ represents an $M \times 1$-dimensional vector of 1's, and $\mathbf{I}$ denotes an $M \times M$-dimensional identity matrix. For the upper-sided TEWMA $\bar{X}$ chart, it is easy to verify that the standard upper-

truncated variable

$$\bar{Z}_t^+ = \frac{\bar{S}_t^+ - E(\bar{S}_t^+)}{\sqrt{V(\bar{S}_t^+)}} \geq \frac{\mu_M - E(\bar{S}_t^+)}{\sqrt{V(\bar{S}_t^+)}} \tag{24}$$

Furthermore, if we define $\left(\mu_M - E(\bar{S}_t^+)\right)/\sqrt{V(\bar{S}_t^+)} = H_U^+$, the in-control region can be denoted as $[H_U^+, H^+]$, where H^+ is the upper control limit of the scheme. Based on the fact that the width of each subinterval is $\Delta^+ = (H^+ - H_U^+)/M$, the midpoint value $L_i^+ = H_U^+ + (i - \Delta^+/2)$ of each subinterval is considered to approximate the transient state i of the charting statistic Q_t^+ at sampling point$t$, where $i = 1, 2, \cdots, M$. Furthermore, the transient probability elements $q_{i,j}$ of $\mathbf{Q}$ can be computed using

$$\begin{aligned} q_{i,j} &= \Pr\left(Q_t^+ \in \text{State } j \;\middle|\; Q_{t-1}^+ \in \text{State } i\right) \\ &= \Pr\left(L_j^+ - \frac{\Delta^+}{2} < Q_t^+ \leqslant L_j^+ + \frac{\Delta^+}{2} \middle| Q_{t-1}^+ = L_i^+\right) \end{aligned} \tag{25}$$

After some algebraic operations, the transient probability elements $q_{i,j}$ are given as follows:

$$\begin{aligned} q_{i,j} &= \Pr\left(L_i^+ + \frac{L_j^+ - L_i^+ - \frac{\Delta^+}{2}}{\lambda} < Z_t^+ \leq L_i^+ + \frac{L_j^+ - L_i^+ + \frac{\Delta^+}{2}}{\lambda}\right) \\ &= \Pr\left(E(\bar{S}_t^+) + \sqrt{V(\bar{S}_t^+)}\left(L_i^+ + \frac{L_j^+ - L_i^+ - \frac{\Delta^+}{2}}{\lambda}\right) < S_t^+ \leq E(\bar{S}_t^+) + \right. \\ &\quad \left. \sqrt{V(\bar{S}_t^+)}\left(L_i^+ + \frac{L_j^+ - L_i^+ + \frac{\Delta^+}{2}}{\lambda}\right)\right) \end{aligned} \tag{26}$$

where $E(\bar{S}_t^+)$ and $V(\bar{S}_t^+)$ can be obtained from Equations (15) and (16), respectively. For the upper-sided TEWMA $\bar{X}$ chart, if we define

$$A_1 = E(\bar{S}_t^+) + \sqrt{V(\bar{S}_t^+)}\left(L_i^+ + \frac{L_j^+ - L_i^+ - \frac{\Delta^+}{2}}{\lambda}\right) \tag{27}$$

$$A_2 = E(\bar{S}_t^+) + \sqrt{V(\bar{S}_t^+)}\left(L_i^+ + \frac{L_j^+ - L_i^+ + \frac{\Delta^+}{2}}{\lambda}\right) \tag{28}$$

then, the transient probability elements $q_{i,j}$ of matrix $\mathbf{Q}$ can be calculated using the following equations,

$$q_{i,j} = \begin{cases} 0 & A_2 < \mu_M \\ \Phi(A_2 - \delta_M) & A_1 < \mu_M \text{ and } A_2 > \mu_M \\ \Phi(A_2 - \delta_M) - \Phi(A_1 - \delta_M) & A_1 > \mu_M \text{ and } A_2 > \mu_M \end{cases} \tag{29}$$

where

$$\delta_M = \frac{\sqrt{n}B\delta\sigma_0}{\sqrt{B^2\sigma_0^2 + \frac{\sigma_M^2}{m}}} \tag{30}$$

and $\Phi(\cdot)$ represents the c.d.f. of the standard normal distribution $N(0,1)$, δ is the magnitude of the standardized mean shift, n is the sample size, and m denotes the number of measurement operations.

Finally, for the initial probability vector $\mathbf{p}$, the elements p_j could be obtained as follows:

$$p_j = \begin{cases} 1, & L_j^+ - \dfrac{\Delta^+}{2} < Q_0^+ \leq L_j^+ + \dfrac{\Delta^+}{2} \\ 0, & \text{otherwise} \end{cases} \tag{31}$$

where $Q_0^+ = E(Z_t^+) = 0$.

4 Effect of measurement errors on the one-sided TEWMA $\bar{X}$ chart

As one of the most extensively used RL characteristics for control chart, the ARL is defined as the average number of observations required for the scheme to trigger a signal. Generally, investigators believe that the smaller the out-of-control ARL (named as ARL_1), the better the performance of the control chart. Hence, when designing a control chart, an acceptable in-control ARL (i.e., ARL_0) should be specified firstly at the beginning of the process monitoring, and then the aim of this scheme is to obtain the minimum ARL_1 (denoted as ARL_{min}) for a predetermined mean shift value δ_{opt}. In this paper, the following optimal design procedure is given for searching the optimal design parameters λ_* and H_*^+ of the upper-sided TEWMA $\bar{X}$ chart with measurement errors, say:

$$\begin{cases} \{\lambda_*, H_*^+\} = \underset{\{\lambda, H^+\}}{\arg\min}\, \mathrm{ARL}_1(B, \eta, \lambda, H^+, m, n, \delta_{opt}) \\ \text{Subject to :} \\ \mathrm{ARL}(B, \eta, \lambda, H^+, m, n, \delta_{opt} = 0) = \mathrm{ARL}_0 \end{cases} \tag{32}$$

where $\eta = \sigma_M/\sigma_0$ is a commonly considered index (namely, the ratio of the standard deviation of measurement error σ_M and the in-control standard deviation σ_0 of the process, hereafter denoted as the standard deviation ratio) for evaluating the effect of measurement errors on the performance of the control chart. With the constraint on the desired $\mathrm{ARL}_0 = 370$, the ARL performance of the upper-sided TEWMA $\bar{X}$ chart is discussed here for illustration. According to the optimal design procedure described in (32), the optimal design parameters $\{\lambda_*, H_*^+\}$ of the upper-sided TEWMA $\bar{X}$ chart are listed in Table 1, for different prespecified mean shifts $\delta_{opt} \in \{0.1, 0.25, 0.5, 0.75, 1, 1.5, 2, 2.5, 3\}$, when $A = 0$, $B = 1$, $\mu_0 = 0$, $\sigma_0 = 1$, $\sigma_M = 1$, $m \in \{1, 6\}$ and $n \in \{3, 5, 7, 9\}$.

(Please insert Table 1 here)

Before investigating the effect of measurement errors on the ARL performance of the upper-sided TEWMA $\bar{X}$ chart, some comparisons of ARL computed using the proposed Markov chain model and the Monte Carlo simulation are given in Table 2. Due to the space limitation, only four sets of optimal design parameters $\{\lambda_*, H_*^+\}$ are provided here for illustration. For instance, when $\delta_{opt} = 0.1$, $m = 1$, $n = \{3, 7\}$, the optimal design parameters of the proposed scheme are $\{\lambda_*, H_*^+\} = \{0.0716, 0.5011\}$ and $\{0.2281, 1.1949\}$, respectively. Meanwhile, when $\delta_{opt} = 1.0$, $m = 6$, $n = \{5, 9\}$, the corresponding optimal design parameters are $\{\lambda_*, H_*^+\} = \{0.3212, 1.5486\}$ and $\{0.5793, 2.4770\}$, respectively. It is noted that the number M of subintervals used in the Markov chain model is 500, and the number of runs employed in the Monte carlo simulation is 5×10^4. As we can see from Table 2, the largest discrepancy among the presented results is less than 1% of the ARL_{min}. This fact means that the Markov chain model established in this study can be satisfactorily verified with the Monte Carlo simulation, and this confirms that the Markov chain model is effective.

(Please insert Table 2 here)

With the constraint on the $\mathrm{ARL}_0 = 370$, the ARL_1 performance of the upper-sided TEWMA $\bar{X}$ chart with the measurement errors is investigated, for several prespecified standard deviation ratios $\eta \in \{0, 0.1, 0.2, 0.3, 0.4, 0.5, 0.6, 0.7, 0.8, 0.9, 1\}$, by setting fixed value of $m \in \{1, 6\}$, $\delta_{opt} = 0.5$, and $n \in \{3, 5, 7, 9\}$. As it can be seen from Figure 1, for the fixed value of n, the ARL_1 values of the upper-sided TEWMA $\bar{X}$ chart with measurement errors are generally larger than the ARL_1 value of the scheme with no measurement error (i.e., the standard deviation ratio $\eta = 0$). Additionally, it can

be observed that the ARL_1 values increase as the standard deviation ratio η increases. For instance, in the case of $m = 1$, when there is no measurement error in the process, the ARL_1 value is 10.46 for $n = 3$, but as the standard deviation ratio η increase from 0.4 to 0.9, the corresponding ARL_1 values of the scheme increases from 11.20 to 16.50, respectively. Similar results can also be observed in the case of $m = 6$, but the increasing trend of ARL_1 is significantly smaller than that in the case of $m = 1$. According to the results presented above, we can draw a conclusion that with the increase of the standard deviation ratio η, the detective efficiency of the scheme can be strongly affected.

(Please insert Figure 1 here)

Not only the standard deviation ratio η, but the effect of B on the performance of the scheme is also investigated in this paper. The ARL_1 performances of the upper-sided TEWMA $\bar{X}$ chart with measurement errors are given in Figure 2, for different values of $B \in \{0.1, 0.2, 0.3, 0.4, 0.5, 0.75, 0.85, 1, 1.5, 2, 2.5, 3, 3.5, 4, 4.5, 5\}$, by setting fixed value of $m \in \{1, 6\}$, $\eta = 1$, $\delta_{opt} = 0.5$, and $n \in \{3, 5, 7, 9\}$. As we can see from Figure 2, for a fixed value of n, when the value of B is smaller than 1, the change of parameter B has a significant effect on the ARL_1 performance of the scheme. Contrarily, if the value of B is greater than 1, the effect of B on ARL_1 is relatively small . For example, in the case of $m = 1$ and $n = 3$, when B changes from 0.2 to 0.5, the corresponding ARL_1 values decreases from 136.07 to 32.39. However, for $m = 1$ and $n = 5$, if B changes from 2 to 3, the corresponding ARL_1 values only shifts from 8.31 to 7.67. Similar results can also be obtained in the case of $m = 6$. Without loss of generality, in terms of the overall performance of the scheme, it can be concluded that for a fixed value of n, if the value of B increases, the negative effect of measurement errors on the upper-sided TEWMA $\bar{X}$ chart gradually decreases until it is comparable to the case of no measurement error.

(Please insert Figure 2 here)

Whatever Figures 1 or 2, the same phenomenon can be observed that the use of multiple measurements can effectively reduce the negative effect of measurement errors on the upper-sided TEWMA $\bar{X}$ chart. For instance, from Figure 1, when a fixed n is selected, with $m = 6$ measurements per item, the upper-sided TEWMA $\bar{X}$ chart has almost similar properties for all values of η, and the negative effect of measurement errors on the scheme can be overlooked. This fact motivates us to further investigate

the effect of multiple measurements m on the detecting performance of the upper-sided TEWMA $\bar{X}$ chart. In this context, Figure 3 illustrates the ARL_1 performance of the upper-sided TEWMA $\bar{X}$ chart for different measurement operations $m \in \{1, 2, 3, 4, 5, 6, 7, 8, 9, 10\}$, when $B = 1$, $\eta = 1$, $\delta_{opt} = 0.5$, and $n \in \{3, 5, 7, 9\}$. According to our observation from Figure 3, as the values of measurements m increases, the negative effect of measurement error on the upper-sided TEWMA $\bar{X}$ chart decreases, especially when m varies from 1 to 2, the results are most significant. For instance, in the case of $n = 3$, when m changes from 1 to 2, the ARL_1 value of the upper-sided TEWMA $\bar{X}$ chart decreases from 20.70 to 13.93. It is worth noting that taking multiple measurements is a good idea to diminish the negative effect of measurements errors on the one-sided TEWMA $\bar{X}$ chart, but the extra costs and time associated with it should also be considered.

(Please insert Figure 3 here)

5 Effect of measurement errors on performance comparison of one-sided EWMA-type charts

The goal of this section is to investigate the effect of measurement errors on ARL performance comparison of one-sided EWMA-type charts, more specifically, the one-sided REWMA $\bar{X}$ chart is introduced here for comparison with the one-sided TEWMA $\bar{X}$ chart in the presence of measurement errors. To provide a fair comparison, these two schemes are investigated in the same condition: for instance, both ARL_0 values of these two schemes are set as 370. Also, the ARL values for the one-sided REWMA $\bar{X}$ chart are computed using the Markov chain model, rather than the Monte Carlo simulation or the integral equation method.

5.1 The one-sided REWMA $\bar{X}$ chart with measurement errors

As a competing scheme, the one-sided REWMA $\bar{X}$ chart is introduced here for detecting process mean shifts. Based on Gan (1993a), the charting statistics of the one-sided REWMA $\bar{X}$ chart with measurement errors can be respectively given as follows:

- In the presence of measurement errors, the charting statistic W_t^+ of the upper-sided REWMA

$\bar{X}$ chart is written as:

$$W_t^+ = \max\left(B_U, \lambda\bar{S}_t + (1-\lambda)W_{t-1}^+\right) \tag{33}$$

- For downward shift detection, the charting statistic W_t^- of the lower-sided REWMA $\bar{X}$ chart with measurement errors can be given as:

$$W_t^- = \min\left(B_L, \lambda\bar{S}_t + (1-\lambda)W_{t-1}^-\right) \tag{34}$$

where $\bar{S}_t$ is defined in Equation (11), B_U and B_L are the reflecting boundaries of the upper- and lower-sided REWMA $\bar{X}$ charts, respectively. Commonly, the reflecting boundary values of the one-sided REWMA $\bar{X}$ chart can be defined as $B_U = B_L = E(\bar{S}_t)$. For the process monitoring, if the charting statistic W_t^+ (W_t^-) exceeds (or falls below) the upper (lower) control limit h^+ (h^-), the one-sided REWMA $\bar{X}$ chart triggers an out-of-control signal, and then the corresponding corrective action(s) should be taken to remove the assignable cause(s). In the presence of measurement errors, the Markov chain model of the upper-sided REWMA $\bar{X}$ chart is also established here for providing a fair comparison with the upper-sided TEWMA $\bar{X}$ chart. Due to the space limitation, reader can see Appendix B for more detail.

5.2 Performance comparison under measurement errors

The goal of this section is to show how the measurement errors affect the ARL performance of one-sided EWMA-type schemes in comparative studies. More specifically, we compare the ARL performance of the upper-sided TEWMA $\bar{X}$ and REWMA $\bar{X}$ charts in the absence and presence of measurement errors. To provide a fair comparison, the number M of subintervals of these two charts is defined as 500. Meanwhile, the same optimal design procedure is used in this section for searching the optimal design parameters of the scheme, and the prespecified mean shifts $\delta_{opt} = \{0.5, 1\}$ are given for illustration.

In order to show the effect of measurement errors in comparative studies, Tables 3 and 4 respectively present the ARL_1 values of the upper-sided TEWMA $\bar{X}$ and REWMA $\bar{X}$ charts for detecting different mean shift values $\delta \in \{0.1, 0.3, 0.5, 0.7, 1, 1.3, 1.5, 1.7, 2, 2.5\}$, when $m = \{1, 6\}$,

$n \in \{3, 5, 7, 9\}$, and $\delta_{opt} \in \{0.5, 1\}$. Furthermore, according to the optimal design procedures mentioned above, the optimal design parameters of these two charts can be searched. For example, for Table 4, when $m = 1$, $n = 3$ and $\delta_{opt} = 0.5$, the optimal design parameters of these two charts with measurement errors are $\{\lambda_*, H_*^+\} = \{0.1220, 0.7484\}$ and $\{\lambda_*, h_*^+\} = \{0.1483, 0.7673\}$. Meanwhile, the corresponding parameters in the absence of measurement errors are $\{\lambda_*, H_*^+\} = \{0.0950, 0.6207\}$ and $\{\lambda_*, h_*^+\} = \{0.1554, 0.7896\}$, respectively. To sum up, as we can see from Tables 3 and 4, the following conclusions can be drawn:

- Firstly, as we can see from those ARL_1 values presented in Tables 3 and 4, regardless of measurement error, the upper-sided TEWMA $\bar{X}$ chart performs better than the upper-sided REWMA $\bar{X}$ chart in terms of the overall detection effectiveness.

- Additionally, no matter for the upper-sided TEWMA $\bar{X}$ chart or the upper-sided REWMA $\bar{X}$ chart, if the scheme does not take multiple measurement operations per item in each sample (i.e., $m = 1$ in this paper), there will be a significant difference between ARL_1 values with and without measurement errors. For example, for the upper-sided TEWMA $\bar{X}$ chart, when $m = 1$, $n = 3$, and $\delta_{opt} = 0.5$, the ARL_1 values with and without measurement errors are 154.53 and 105.66 for $\delta = 0.1$.

- On the other hand, by observing from Tables 3 and 4, it is easy to know that, taking multiple measurement operation can not only reduce the negative effect of measurement errors on both schemes, but this approach also reduces the difference between ARL_1 values in the presence and absence of measurement errors. For example, for the upper-sided TEWMA $\bar{X}$ chart, when $m = 1$, $n = 3$, and $\delta_{opt} = 0.5$, the ARL_1 values with and without measurement errors are 154.53 and 105.66 for $\delta = 0.1$. But when $m = 6$, $n = 3$, and $\delta_{opt} = 0.5$, the corresponding ARL_1 values are 117.54 and 110.41 for $\delta = 0.1$.

(Please insert Tables 3 and 4 here)

The above conclusions verify the following facts again that, in the comparative studies, irrespective of the δ_{opt} value, taking multiple measurement operation will reduce the negative effect of measurement errors on both the one-sided TEWMA $\bar{X}$ chart and one-sided REWMA $\bar{X}$ chart. Meanwhile, relative

to m, the value of n has a little effect on the overall performance of these two charts in comparative studies.

Furthermore, the ARL_{min} performance of the upper-sided TEWMA $\bar{X}$ chart and upper-sided REWMA $\bar{X}$ charts for prespecified mean shift values $\delta_{opt} \in \{0.1, 0.25, 0.5, 0.75, 1, 1.5, 2, 2.5, 3\}$ are also illustrated here to study the effect of measurement errors in comparative studies, where Table 5 lists the ARL_{min} performance of these two schemes in the absence of measurement errors (i.e., $A = 0$, $B = 1$, $\sigma_M = 0$). For instance, when $m = 1$, $n = 5$, and $\delta_{opt} = 0.5$, the ARL_{min} value of the upper-sided TEWMA $\bar{X}$ and upper-sided REWMA $\bar{X}$ charts are 7.0200 and 7.6289, respectively. Meanwhile, Table 6 presents the corresponding ARL_1 performance of these two schemes in the presence of measurement errors (i.e., $A = 0$, $B = 1$, $\sigma_M = 1$), for example, when $m = 6$, $n = 3$, and $\delta_{opt} = 1$, the ARL_{min} value of the upper-sided TEWMA $\bar{X}$ and upper-sided $\bar{X}$ REWMA charts are 4.0253 and 4.4039, respectively.

(Please insert Tables 5 and 6 here)

Through the analysis of the ARL performance in Tables 5 and 6, it is not difficult to find that when there is no measurement error in the monitoring process (although some studies are often carried out based on this assumption, it is almost impossible to occur in the actual process), the upper-sided TEWMA $\bar{X}$ chart using the optimal design parameters is uniformly superior to the corresponding upper-sided REWMA $\bar{X}$ chart. But when the measurement errors exist in the monitoring process (this situation is relatively more common in the actual process), the ARL_{min} performance comparison in some circumstances (most one occur when $m = 1$, but none in the case of $m > 1$) is contrary to the above conclusion that "the upper-sided TEWMA $\bar{X}$ chart performs better than the upper-sided REWMA $\bar{X}$ chart". For instance, when $m = 1$, $n = 3$, and $\delta_{opt} = 0.5$, for the case without measurement errors, the upper-sided TEWMA $\bar{X}$ chart performs better than the upper-sided REWMA $\bar{X}$ chart, but under the same condition, for the case with measurement errors, the ARL_{min} value of the upper-sided TEWMA $\bar{X}$ chart is lager than the corresponding ARL_{min} value of the upper-sided REWMA $\bar{X}$ chart.

In summary, although there are some negative effects, the presence of measurement errors does

not change the conclusion that the one-sided TEWMA $\bar{X}$ chart is more efficient than the one-sided REWMA $\bar{X}$ chart for detecting mean shifts, especially in the case where multiple measurement operations are considered.

6 A numerical example

A 125 g yogurt cup filling process adapted from Costa & Castagliola (2011) is used here to illustrate the implementation of the one-sided TEWMA $\bar{X}$ chart in detecting process mean shifts, where the quality characteristic Y_t is the weight of each yogurt cup. This example is also employed in many studies involving measurement errors, for example, in Cheng & Wang (2018) and Saha et al. (2022). Before starting the process monitoring, the in-control mean $\mu_0 = 124.9$ and the in-control standard deviation $\sigma_0 = 0.76$ have been respectively estimated in Phase I. The standard deviation of measurement error $\sigma_M = 0.24$ can be estimated from an independent R&R (Repeatability and Reproducibility) research. Based on this parameter, the standard deviation ratio η is equal to $\sigma_M/\sigma_0 = 0.24/0.76 = 0.316$. Meanwhile, for the linear covariate error model, the parameters $A = 0$ and $B = 1$ corresponding to the most common scenario are used in this example.

As it can be obtained from Costa & Castagliola (2011), the practitioner in charge of this process decides to take $n = 5$ yogurt cups every hours, and then taking $m = 2$ independent measurement operations per item. In this example, the first 10 subgroups are measured from in-control situation, where the data used directly from Cheng & Wang (2018). Then, the last 10 subgroups are considered as out-of-control, see column 2 to 11 in Table 7. In addition, the sample mean values $\bar{Y}$ are also listed in column 12 of Table 7. During process monitoring, the practitioner pays more attention to the scenario that the product is less than the process mean. This means that the lower-sided scheme is suitable for monitoring this yogurt cup filling process. Furthermore, let us assume that the practitioner are interested in detecting a prespecified small downward shift $0.5 \times \theta_0$. According to the optimal design procedure introduced above, the lower-sided TEWMA $\bar{X}$ chart with the optimal design parameters $\{\lambda_*, H_*^-\} = \{0.1978, -0.9515\}$, and the lower-sided REWMA $\bar{X}$ chart with the optimal design parameters $\{\lambda_*, h_*^-\} = \{0.1748, -0.7746\}$ are employed here for process monitoring.

(Please insert Table 7 here)

As we can see from Table 7, all charting statistics of these two schemes are listed in columns 13 and 14, respectively. It should be noted that, for these two lower-sided schemes, an out-of-control signal is triggered when the charting statistic falls below the corresponding lower control limit. For instance, when $t = 15$, the charting statistic W_t^- of the lower-sided TEWMA $\bar{X}$ chart falls below the control limit H_*^-, and then an out-of-control signal is given and the corresponding actions should be taken to identify and remove the downward mean shift. Meanwhile, the charting statistic Q_t^- of the lower-sided REWMA $\bar{X}$ chart generates an out-of-control signal at $t = 19$ observation. Furthermore, all these two scheme are shown in Figure 4 for illustrating the detailed monitoring process.

(Please insert Figure 4 here)

7 Conclusion

In this paper, the effect of measurement errors on the one-sided TEWMA $\bar{X}$ chart with linear covariate error model was investigated. Meanwhile, a Markov chain model was established to evaluate the RL properties of the suggested scheme in the presence of measurement errors. Furthermore, an optimal design procedure was given to search the optimal design parameters of the scheme. According to the presented results, the efficiency of the one-sided TEWMA $\bar{X}$ chart with measurement errors is strongly affected compared to the case with no measurement error. To compensate for the negative effect of measurement errors, it is suggested to take multiple measurement operations per item in each sample. Finally, in the presence of measurement errors, the ARL performance of the one-sided TEWMA $\bar{X}$ chart was compared with that of the conventional one-sided REWMA $\bar{X}$ chart, and the conclusions from the presented results shown that, regardless of the presence or absence of measurement errors, the one-sided TEWMA $\bar{X}$ chart had a better overall ARL performance than the one-sided REWMA $\bar{X}$ chart. In addition, irrespective of the δ_{opt} value, taking multiple measurement operation can significantly reduce the negative effect of measurement errors on both the one-sided TEWMA $\bar{X}$ chart and one-sided REWMA $\bar{X}$ chart. Besides, relative to m, the sample size n has little effect on the overall performance of these two charts in comparative studies.

In this paper, the upper- and lower-truncated variables $\bar{X}_t^+$ and $\bar{X}_t^-$ are all built based on the truncation point μ_0. However, μ_0 is not always the best choice for process monitoring. Similarly, for the one-sided REWMA $\bar{X}$ chart, the best value of reflecting boundary is not always $E(\bar{X}_t)$. Therefore, a possible future extension for the current research is to investigate the effect of measurement errors on the one-sided TEWMA $\bar{X}$ chart (or the one-sided REWMA $\bar{X}$ chart) with the optimized truncation point (the optimized reflecting boundary). Furthermore, using real-life data to demonstrate the implementation of control charts, for example, as done in Netshiozwi et al. (2023), will be more persuasive than the simulated ones.

Disclosure statement

No potential conflict of interest was reported by the author(s).

Funding

This work was supported by the National Natural Science Foundation of China under Grant 72301130, 72101123; Scientific Research Foundation of Nanjing Institute of Technology under Grant YKJ202308; Humanity and Social Science Foundation of Ministry of Education of China under Grant 19YJA630061; Natural Science Foundation of Jiangsu Province under Grant BK20200750; Nanjing Science and Technology Innovation Project for Overseas Educators under Grant NJKCZYZZ2022-08.

References

Bennett, C. A. (1954). Effect of measurement error on chemical process control. *Industrial Quality Control*, *10*, 17–20.

Castagliola, P., Maravelakis, P. E., & Figueiredo, F. O. (2016). The EWMA median chart with estimated parameters. *IIE Transactions*, *48*, 66–74.

Cheng, X., & Wang, F. (2018). The performance of EWMA median and CUSUM median control charts for a normal process with measurement errors. *Quality and Reliability Engineering International*, *34*, 203–213.

Chiu, J., & Tsai, C. (2013). Properties and performance of one-sided cumulative count of conforming chart with parameter estimation in high-quality processes. *Journal of Applied Statistics*, *40*, 2341–2353.

Costa, A. F., & Castagliola, P. (2011). Effect of measurement error and autocorrelation on the $\bar{X}$ chart. *Journal of Applied Statistics*, *38*, 661–673.

Dickinson, R. M., Roberts, D. A. O., Driscoll, A. R., Woodall, W. H., & Vining, G. G. (2014). CUSUM charts for monitoring the characteristic life of censored Weibull lifetimes. *Journal of Quality Technology*, *46*, 340–358.

Gan, F. (1993a). Exponentially weighted moving average control charts with reflecting boundaries. *Journal of Statistical Computation and Simulation*, *46*, 45–67.

Gan, F. (1993b). An optimal design of ewma control charts based on median run length. *Journal of Statistical Computation and Simulation*, *45*, 169–184.

García-Bustos, S., & Zambrano, G. (2022). Control charts for health surveillance based on residuals of negative binomial regression. *Quality and Reliability Engineering International*, *38*, 2521–2532.

Haq, A. (2020). One-sided and two one-sided MEWMA charts for monitoring process mean. *Journal of Statistical Computation and Simulation*, *90*, 699–718.

Haq, A., Brown, J., Moltchanova, E., & Al-Omari, A. I. (2015). Effect of measurement error on exponentially weighted moving average control charts under ranked set sampling schemes. *Journal of Statistical Computation and Simulation*, *85*, 1224–1246.

Hossain, M. P., Sanusi, R. A., Omar, M. H., & Riaz, M. (2019). On designing maxwell CUSUM control chart: an efficient way to monitor failure rates in boring processes. *The International Journal of Advanced Manufacturing Technology*, *100*, 1923–1930.

Hu, X., Qiao, Y., Zhou, P., Zhong, J., & Wu, S. (2023). Modified one-sided EWMA charts for monitoring time between events. *Communications in Statistics–Simulation and Computation*, *52*, 1041–1056.

Khati Dizabadi, A., Shahrokhi, M., & Maleki, M. R. (2016). On the effect of measurement error with linearly increasing-type variance on simultaneous monitoring of process mean and variability. *Quality and Reliability Engineering International*, *32*, 1693–1705.

Li, Y., Qin, J., & Wu, C. (2023). A robust adaptive exponentially weighted moving average control chart with a distribution-free design strategy. *Computers & Industrial Engineering*, *177*, 109083.

Li, Z., Zou, C., Gong, Z., & Wang, Z. (2014). The computation of average run length and average time to signal: an overview. *Journal of Statistical Computation and Simulation*, *84*, 1779–1802.

Linna, K. W., & Woodall, W. H. (2001). Effect of measurement error on Shewhart control charts. *Journal of Quality Technology*, *33*, 213–222.

Maleki, M. R., Amiri, A., & Castagliola, P. (2017). Measurement errors in statistical process monitoring: A literature review. *Computers & Industrial Engineering*, *103*, 316–329.

Maravelakis, P. E. (2012). Measurement error effect on the CUSUM control chart. *Journal of Applied Statistics*, *39*, 323–336.

Montgomery, D. C. (2012). *Introduction to statistical quality control*. (Seventh ed.). New York: John Wiley & Sons.

Montgomery, D. C., & Runger, G. C. (1993). Gauge capability and designed experiments. Part I: basic methods. *Quality Engineering*, *6*, 115–135.

Mukherjee, A., & Marozzi, M. (2021). Nonparametric Phase-II control charts for monitoring high-dimensional processes with unknown parameters. *Journal of Quality Technology*, *54*, 44–64.

Netshiozwi, U., Yeganeh, A., Shongwe, S. C., & Hakimi, A. (2023). Data-Driven Surveillance of Internet Usage Using a Polynomial Profile Monitoring Scheme. *Mathematics*, *11*, 3650.

Nguyen, H. D., Tran, K. P., Celano, G., Maravelakis, P. E., & Castagliola, P. (2020). On the effect of the measurement error on Shewhart t and EWMA t control charts. *The International Journal of Advanced Manufacturing Technology*, *107*, 4317–4332.

Noor-ul-Amin, M., & Riaz, A. (2021). Performance of adaptive exponentially weighted moving average control chart in the presence of measurement error. *Journal of Statistical Computation and Simulation*, *91*, 2328–2343.

Perry, M. B. (2020). An EWMA control chart for categorical processes with applications to social network monitoring. *Journal of Quality Technology*, *52*, 182–197.

Saha, S., Khoo, M. B., Abubakar, S. S., Das, U. K., & Lee, M. H. (2022). A new EWMA median chart with measurement errors in short production runs–An application in yogurt cup filling process. *Quality and Reliability Engineering International*, *38*, 1994–2014.

Schaffer, J. R., & Kim, M. (2007). Number of replications required in control chart Monte Carlo simulation studies. *Communications in Statistics–Simulation and Computation*, *36*, 1075–1087.

Shu, L., & Jiang, W. (2006). A Markov chain model for the adaptive CUSUM control chart. *Journal of Quality Technology*, *38*, 135–147.

Shu, L., Jiang, W., & Wu, S. (2007). A one-sided EWMA control chart for monitoring process means. *Communications in Statistics–Simulation and Computation*, *36*, 901–920.

Tang, A., Castagliola, P., Sun, J., & Hu, X. (2018). The effect of measurement errors on the adaptive EWMA chart. *Quality and Reliability Engineering International*, *34*, 609–630.

Tran, K. D., Nguyen, H. D., Nguyen, T. H., & Tran, K. P. (2021). Design of a variable sampling interval exponentially weighted moving average median control chart in presence of measurement errors. *Quality and Reliability Engineering International*, *37*, 374–390.

Xie, F., Castagliola, P., Li, Z., Sun, J., & Hu, X. (2022a). One-sided adaptive truncated exponentially weighted moving average $\bar{X}$ schemes for detecting process mean shifts. *Quality Technology & Quantitative Management*, *19*, 533–561.

Xie, F., Castagliola, P., Qiao, Y., Hu, X., & Sun, J. (2022b). A one-sided exponentially weighted moving average control chart for time between events. *Journal of Applied Statistics*, *49*, 3928–3957.

Yang, S., & Jiang, T. (2019). Service quality variation monitoring using the interquartile range control chart. *Quality Technology & Quantitative Management*, *16*, 613–627.

Appendix A

Let us assume that the random variable X follows a normal distribution $N(\mu_0, \sigma_0^2)$. Also, let us denote $\phi(x, \mu_0, \sigma_0^2)$ and $\Phi(x, \mu_0, \sigma_0^2)$ as the probability density function (p.d.f.) and the cumulative distribution function (c.d.f.) of the normal distribution $N(\mu_0, \sigma_0^2)$, respectively. Meanwhile, simplify $\phi(x) = \phi(x, 0, 1)$ and $\Phi(x) = \Phi(x, 0, 1)$ to be their standardized counterparts. If the upper truncated random variable $X^+ = \max(c, X)$ is given, where c is a truncation point. It is not difficult to prove that the p.d.f. $f_{X^+}(x, \mu_0, \sigma_0^2, c)$ of X^+ is equal to

$$f_{X^+}(x, \mu_0, \sigma_0^2, c) = \Phi(c, \mu_0, \sigma_0^2) \times I(x = c) + \phi(x, \mu_0, \sigma_0^2) \times I(x > c)$$

where $I(K)$ is an indicator function that is equal to 1 if the condition K holds and 0 otherwise. By definition, the expectance $E(X^+)$ of X^+ is equal to

$$E(X^+) = c \times \Phi(c, \mu_0, \sigma_0^2) + \int_c^{+\infty} x\phi(x, \mu_0, \sigma_0^2)\mathrm{d}x$$

For more details about the integral $\int_c^{+\infty} x\phi(x, \mu_0, \sigma_0^2)\mathrm{d}x$ in the above equation, we can give it as,

$$\begin{aligned}
\int_c^{+\infty} x\phi(x, \mu_0, \sigma_0^2)\mathrm{d}x &= \int_c^{+\infty} (x - \mu_0 + \mu_0)\phi(x, \mu_0, \sigma_0^2)\mathrm{d}x \\
&= \int_c^{+\infty} (x - \mu_0)\phi(x, \mu_0, \sigma_0^2)\mathrm{d}x + \int_c^{+\infty} \mu_0\phi(x, \mu_0, \sigma_0^2)\mathrm{d}x \\
&= -\sigma_0^2 \int_c^{+\infty} \frac{-(x - \mu_0)}{\sigma_0^2}\phi(x, \mu_0, \sigma_0^2)\mathrm{d}x + \mu_0 \int_c^{+\infty} \phi(x, \mu_0, \sigma_0^2)\mathrm{d}x \\
&= -\sigma_0^2 \int_c^{+\infty} \phi'(x, \mu_0, \sigma_0^2)\mathrm{d}x + \mu_0 \left[1 - \Phi(c, \mu_0, \sigma_0^2)\right] \\
&= -\sigma_0^2 \left[\phi(+\infty, \mu_0, \sigma_0^2) - \phi(c, \mu_0, \sigma_0^2)\right] + \mu_0 \left[1 - \Phi(c, \mu_0, \sigma_0^2)\right] \\
&= \sigma_0^2\phi(c, \mu_0, \sigma_0^2) + \mu_0 \left[1 - \Phi(c, \mu_0, \sigma_0^2)\right]
\end{aligned}$$

Hence, the mean $E(X^+)$ of X^+ is,

$$E(X^+) = \mu_0 + (c - \mu_0)\Phi(c, \mu_0, \sigma_0^2) + \phi(c, \mu_0, \sigma_0^2)\sigma_0^2$$

Similar to $E(X^+)$,

$$E((X^+)^2) = c^2\Phi(c, \mu_0, \sigma_0^2) + \int_c^{+\infty} x^2\phi(x, \mu_0, \sigma_0^2)\mathrm{d}x$$

For more details about the integral $\int_c^{+\infty} x^2\phi(x, \mu_0, \sigma_0^2)\mathrm{d}x$, it is not difficult to see that,

$$\begin{aligned}
\int_c^{+\infty} x^2\phi(x, \mu_0, \sigma_0^2)\mathrm{d}x =& \int_c^{+\infty} x(x - \mu_0 + \mu_0)\phi(x, \mu_0, \sigma_0^2)\mathrm{d}x \\
=& \int_c^{+\infty} x(x - \mu_0)\phi(x, \mu_0, \sigma_0^2)\mathrm{d}x + \int_c^{+\infty} x\mu_0\phi(x, \mu_0, \sigma_0^2)\mathrm{d}x \\
=& -\sigma_0^2 \int_c^{+\infty} x\frac{-(x - \mu_0)}{\sigma_0^2}\phi(x, \mu_0, \sigma_0^2)\mathrm{d}x + \mu_0 \int_c^{+\infty} x\phi(x, \mu_0, \sigma_0^2)\mathrm{d}x \\
=& -\sigma_0^2 \int_c^{+\infty} x\phi'(x, \mu_0, \sigma_0^2)\mathrm{d}x + \mu_0 \left\{\sigma_0^2\phi(c, \mu_0, \sigma_0^2) + \mu_0 \left[1 - \Phi(c, \mu_0, \sigma_0^2)\right]\right\} \\
=& -\sigma_0^2 \left[-c\phi(c, \mu_0, \sigma_0^2) - \left(1 - \Phi(c, \mu_0, \sigma_0^2)\right)\right] + \mu_0 \times \\
& \left\{\sigma_0^2\phi(c, \mu_0, \sigma_0^2) + \mu_0 \left[1 - \Phi(c, \mu_0, \sigma_0^2)\right]\right\} \\
=& \mu_0^2 + \sigma_0^2 - (\mu_0^2 + \sigma_0^2)\Phi(c, \mu_0, \sigma_0^2) + (\mu_0 + c)\sigma_0^2\phi(c, \mu_0, \sigma_0^2)
\end{aligned}$$

Based on this,

$$E((X^+)^2) = \mu_0^2 + \sigma_0^2 + \left(c^2 - \mu_0^2 - \sigma_0^2\right)\Phi(c, \mu_0, \sigma_0^2) + (\mu_0 + c)\sigma_0^2\phi(c, \mu_0, \sigma_0^2)$$

Furthermore, the variance $V(X^+)$ of X^+ is,

$$\begin{aligned}
V((X^+)^2) =& E((X^+)^2) - E^2(X^+) \\
=& \left[1 - \Phi(c, \mu_0, \sigma_0^2)\right](\mu_0^2 + \sigma_0^2) + (c + \mu_0)\sigma_0^2\phi(c, \mu_0, \sigma_0^2) + c^2\Phi(c, \mu_0, \sigma_0^2) \\
& - \left[\mu_0 + (c - \mu_0)\Phi(c, \mu_0, \sigma_0^2) + \phi(c, \mu_0, \sigma_0^2)\sigma_0^2\right]^2
\end{aligned}$$

On the other side, for the lower-truncated variable $X^- = \min(c, X)$, the p.d.f. $f_{X^-}(x, \mu_0, \sigma_0^2, c)$ of X^- can be given as

$$f_{X^-}(x, \mu_0, \sigma_0^2, c) = \phi(x, \mu_0, \sigma_0^2) \times I(x < c) + \left[1 - \Phi(c, \mu_0, \sigma_0^2)\right] \times I(x = c)$$

Based on this equation, the expectation $E(X^-)$ of X^- is,

$$E(X^-) = c + (c - \mu_0)\Phi(c, \mu_0, \sigma_0^2) - \phi(c, \mu_0, \sigma_0^2)\sigma_0^2$$

In addition,

$$\begin{aligned} E((X^-)^2) &= c^2[1 - \Phi(c, \mu_0, \sigma_0^2)] + \int_{-\infty}^{c} x^2 \phi(x, \mu_0, \sigma_0^2) \mathrm{d}x \\ &= c^2 + \left(\mu_0^2 + \sigma_0^2 - c^2\right) \Phi(c, \mu_0, \sigma_0^2) - (\mu_0 + c)\sigma_0^2 \phi(c, \mu_0, \sigma_0^2) \end{aligned}$$

Furthermore, the variance $V(X^-)$ of X^- is,

$$\begin{aligned} V((X^-)^2) &= E((X^-)^2) - E^2(X^-) \\ &= c^2 + \left(\mu_0^2 + \sigma_0^2 - c^2\right) \Phi(c, \mu_0, \sigma_0^2) - (\mu_0 + c)\sigma_0^2 \phi(c, \mu_0, \sigma_0^2) \\ &\quad - \left[c + (\mu_0 - c)\Phi(c, \mu_0, \sigma_0^2) - \phi(c, \mu_0, \sigma_0^2)\sigma_0^2\right]^2 \end{aligned}$$

Finally, according to the above derivation, for the standard normally distributed random variable $\bar{S} \sim N(0, 1)$, when $c = \mu_M$, it is not difficult to obtain the mean and variance of the upper- and lower-truncated variables S^+ and S^- in Equations (15) to (18).

Appendix B

Due to the space limitation, only the Markov chain model of the upper-sided REWMA $\bar{X}$ chart, with the presence of measurement errors, is established here for illustration. Similar to the case of upper-sided TEWMA $\bar{X}$ chart, the in-control region of the scheme is also divided into M subintervals. According to Equation (33), the in-control region is denoted as $[B_U, h^+]$, and then the width of each subintervals can be written as $\Delta_R^+ = (h^+ - B_U)/M$. Based on this, the midpoint value $R_i^+ = B_U + (i - \Delta_R^+/2)$ is used here to approximate the transient state i of the charting statistic W_t^+. The

transient probability elements $q'_{i,j}$ in upper-sided REWMA $\bar{X}$ chart are denoted as follows:

$$\begin{aligned} q'_{i,j} =& \Pr\left(W_t^+ \in \text{State } j \;\middle|\; W_{t-1}^+ \in \text{State } i\right) \\ =& \begin{cases} \Pr\left(W_t^+ \leqslant R_j^+ + \frac{\Delta_R^+}{2} \middle| W_{t-1}^+ = R_i^+\right) & j = 1 \\ \Pr\left(R_j^+ - \frac{\Delta_R^+}{2} < W_t^+ \leqslant R_j^+ + \frac{\Delta_R^+}{2} \middle| W_{t-1}^+ = R_i^+\right) & j = 2, 3, \cdots, M \end{cases} \end{aligned}$$

After some algebraic operations, the transient probability elements $q'_{i,j}$ can be written as follows:

$$q'_{i,j} = \begin{cases} \Pr\left(\bar{S}_t \leqslant R_i^+ + \frac{R_j^+ - R_i^+ + \Delta_R^+/2}{\lambda}\right) & j = 1 \\ \Pr\left(R_i^+ + \frac{R_j^+ - R_i^+ - \Delta_R^+/2}{\lambda} < \bar{S}_t \leqslant R_i^+ + \frac{R_j^+ - R_i^+ + \Delta_R^+/2}{\lambda}\right) & j = 2, 3, \cdots, M \end{cases}$$

If we set the following variables as

$$\begin{aligned} U_1 &= R_i^+ + \frac{R_j^+ - R_i^+ - \Delta_R^+/2}{\lambda} \\ U_2 &= R_i^+ + \frac{R_j^+ - R_i^+ + \Delta_R^+/2}{\lambda} \end{aligned}$$

the transient probability elements $q'_{i,j}$ of matrix $\mathbf{Q}'$ can be defined as follows:

$$q'_{i,j} = \begin{cases} \Phi(U_2 - \delta_M) & j = 1 \\ \Phi(U_2 - \delta_M) - \Phi(U_1 - \delta_M) & j = 2, 3, \cdots, M \end{cases}$$

where δ_M has been defined in Equation (30). Additionally, the elements of initial probability vector $\mathbf{p}'$ is:

$$p'_j = \begin{cases} 1, & R_j^+ - \dfrac{\Delta_R^+}{2} < W_0^+ \leq R_j^+ + \dfrac{\Delta_R^+}{2} \\ 0, & \text{otherwise} \end{cases} \tag{A.1}$$

where $W_0^+ = E(\bar{S}_t) = 0$. Finally, the ARL value of the upper-sided REWMA $\bar{X}$ chart can be computed using $\text{ARL} = \mathbf{p}'^{\mathsf{T}}(\mathbf{I} - \mathbf{Q}')^{-1}\mathbf{1}$.

Table 1: The optimal design parameters $\{\lambda_*, H_*^+\}$ of the upper-sided TEWMA $\bar{X}$ chart for different prespecified mean shifts $\delta_{opt} \in \{0.1, 0.25, 0.5, 0.75, 1, 1.5, 2, 2.5, 3\}$.
($A = 0$, $B = 1$, $\mu_0 = 0$, $\sigma_0 = 1$, $\sigma_M = 1$, $m \in \{1, 6\}$, and $n \in \{3, 5, 7, 9\}$)

m	n		δ_{opt}								
			0.1	0.25	0.5	0.75	1	1.5	2	2.5	3
1	3	λ_*	0.0716	0.1590	0.1792	0.2062	0.1028	0.2677	0.5004	0.6581	0.8353
		H_*^+	0.5011	0.9121	0.9976	1.1077	0.6585	1.3482	2.1944	2.7625	3.4272
	5	λ_*	0.1438	0.0936	0.1066	0.1902	0.3385	0.4731	0.6166	0.8702	0.8735
		H_*^+	0.8464	0.6137	0.6766	1.0429	1.6123	2.0972	2.6115	3.5627	3.5754
	7	λ_*	0.1113	0.0661	0.0980	0.2457	0.3581	0.5441	0.7921	0.8222	0.8853
		H_*^+	0.6985	0.4709	0.6350	1.2635	1.6838	2.3508	3.2618	3.3766	3.6219
	9	λ_*	0.0939	0.1063	0.0938	0.3164	0.3797	0.7082	0.9300	0.9197	0.9326
		H_*^+	0.6149	0.6750	0.6144	1.5309	1.7621	2.9470	3.7988	3.7577	3.8090
6	3	λ_*	0.0135	0.0591	0.1063	0.2772	0.2289	0.4492	0.7361	0.8282	0.8875
		H_*^+	0.1248	0.4320	0.6751	1.3843	1.1981	2.0118	3.0507	3.3998	3.6306
	5	λ_*	0.0716	0.0857	0.2366	0.1990	0.3212	0.7127	0.8587	0.9159	0.9826
		H_*^+	0.5011	0.5739	1.2282	1.0788	1.5486	2.9636	3.5176	3.7424	4.0106
	7	λ_*	0.0241	0.0411	0.1625	0.3081	0.4719	0.7929	0.9336	0.7232	0.8469
		H_*^+	0.2097	0.3253	0.9273	1.5002	2.0928	3.2646	3.8130	3.0025	3.4721
	9	λ_*	0.0716	0.0987	0.0968	0.4221	0.5793	0.8873	0.8757	0.8996	0.9473
		H_*^+	0.5011	0.6386	0.6293	1.9147	2.4770	3.6295	3.5843	3.6782	3.8680

Table 2: ARL_{min} values of the upper-sided TEWMA $\bar{X}$ chart computed using the Markov chain model versus those values obtained using the Monte Carlo simulation.

δ_{opt}	m	n	$\{\lambda, H^+\}$	Monte Carlo	Markov Chain
0.1	1	3	{0.0716,0.5011}	138.0941	137.9637
		7	{0.2281,1.1949}	125.7980	126.2962
1	6	5	{0.3212,1.5486}	2.7347	2.7513
		9	{0.5793,2.4770}	1.7578	1.7540

Table 3: The ARL_1 comparisons between the upper-sided TEWMA $\bar{X}$ chart and the upper-sided REWMA $\bar{X}$ chart in the absence of measurement errors.

m	n	δ_{opt}	Scheme	λ	$H^+(h^+)$	δ									
						0.1	0.3	0.5	0.7	1	1.3	1.5	1.7	2	2.5
1	3	0.5	TEWMA	0.0950	0.6207	105.66	23.05	10.33	6.29	3.89	2.84	2.43	2.14	1.84	1.45
			REWMA	0.1554	0.7896	121.69	25.95	11.16	6.81	4.31	3.19	2.75	2.43	2.11	1.79
		1	TEWMA	0.2879	1.4244	145.43	33.50	12.50	6.56	3.58	2.45	2.04	1.76	1.45	1.15
			REWMA	0.3421	1.2843	153.87	36.55	13.51	7.07	3.90	2.71	2.28	1.98	1.66	1.28
	5	0.5	TEWMA	0.1463	0.8574	89.59	16.40	7.02	4.26	2.69	2.01	1.74	1.52	1.26	1.04
			REWMA	0.2258	0.9923	104.01	18.59	7.63	4.63	2.95	2.24	1.96	1.75	1.47	1.12
		1	TEWMA	0.3978	1.8276	129.11	24.92	8.56	4.40	2.43	1.70	1.43	1.24	1.08	1.01
			REWMA	0.5865	1.8354	152.21	33.59	11.09	5.25	2.65	1.77	1.46	1.26	1.09	1.01
	7	0.5	TEWMA	0.1806	1.0034	78.05	12.79	5.41	3.32	2.15	1.62	1.38	1.20	1.05	1.00
			REWMA	0.3528	1.3096	102.26	16.35	6.09	3.53	2.22	1.66	1.41	1.22	1.06	1.00
		1	TEWMA	0.4357	1.9634	112.79	18.74	6.29	3.31	1.90	1.37	1.18	1.07	1.01	1.00
			REWMA	0.6067	1.8801	132.77	24.58	7.77	3.78	2.02	1.41	1.20	1.08	1.01	1.00
	9	0.5	TEWMA	0.1850	1.0215	66.37	10.28	4.47	2.81	1.86	1.40	1.19	1.07	1.01	1.00
			REWMA	0.3105	1.2086	82.53	12.02	4.87	3.01	1.99	1.51	1.27	1.11	1.02	1.00
		1	TEWMA	0.4062	1.8576	94.17	13.71	4.79	2.68	1.63	1.21	1.08	1.02	1.00	1.00
			REWMA	0.6470	1.9696	121.14	19.97	6.14	3.02	1.67	1.20	1.07	1.02	1.00	1.00
6	3	0.5	TEWMA	0.1133	0.7080	110.41	23.84	10.40	6.23	3.81	2.76	2.36	2.08	1.78	1.39
			REWMA	0.1434	0.7516	118.97	25.39	11.11	6.86	4.38	3.26	2.80	2.48	2.15	1.83
		1	TEWMA	0.2469	1.2681	138.58	31.03	11.83	6.38	3.58	2.49	2.08	1.80	1.50	1.18
			REWMA	0.3330	1.2628	152.68	36.00	13.35	7.03	3.91	2.72	2.29	2.00	1.68	1.30
	5	0.5	TEWMA	0.1255	0.7644	85.27	15.91	7.00	4.31	2.74	2.07	1.79	1.58	1.30	1.05
			REWMA	0.1583	0.7986	92.39	16.92	7.62	4.86	3.20	2.45	2.16	1.96	1.72	1.29
		1	TEWMA	0.3931	1.8105	128.42	24.71	8.51	4.39	2.43	1.70	1.43	1.24	1.08	1.01
			REWMA	0.5060	1.6572	142.64	29.52	9.90	4.91	2.64	1.82	1.52	1.31	1.12	1.01
	7	0.5	TEWMA	0.2171	1.1515	83.64	13.40	5.44	3.27	2.08	1.55	1.32	1.16	1.04	1.00
			REWMA	0.2486	1.0527	88.12	14.09	5.88	3.65	2.40	1.86	1.62	1.40	1.14	1.01
		1	TEWMA	0.4128	1.8815	110.04	18.07	6.16	3.29	1.91	1.38	1.19	1.08	1.01	1.00
			REWMA	0.6321	1.9364	135.60	25.61	8.03	3.84	2.02	1.40	1.19	1.08	1.01	1.00
	9	0.5	TEWMA	0.2280	1.1944	72.18	10.77	4.46	2.75	1.79	1.34	1.15	1.05	1.01	1.00
			REWMA	0.3458	1.2931	86.78	12.58	4.90	2.97	1.94	1.45	1.22	1.09	1.01	1.00
		1	TEWMA	0.4373	1.9691	97.77	14.37	4.90	2.69	1.61	1.20	1.07	1.02	1.00	1.00
			REWMA	0.5480	1.7502	110.16	17.02	5.54	2.93	1.72	1.25	1.10	1.03	1.00	1.00

Table 4: The ARL_1 comparisons between the upper-sided TEWMA $\bar{X}$ chart and the upper-sided REWMA $\bar{X}$ chart in the presence of measurement errors.

m	n	δ_{opt}	Scheme	λ	$H^+(h^+)$	δ									
						0.1	0.3	0.5	0.7	1	1.3	1.5	1.7	2	2.5
1	3	0.5	TEWMA	0.1220	0.7484	154.53	42.39	18.45	10.62	6.12	4.23	3.50	3.00	2.49	1.98
			REWMA	0.1483	0.7673	163.11	45.17	19.45	11.31	6.75	4.81	4.06	3.52	2.95	2.37
		1	TEWMA	0.1028	0.6585	148.81	40.38	17.94	10.52	6.18	4.31	3.58	3.07	2.55	2.04
			REWMA	0.1617	0.8088	165.93	46.49	19.81	11.36	6.69	4.74	3.98	3.45	2.89	2.32
	5	0.5	TEWMA	0.1066	0.6766	119.31	27.27	11.96	7.14	4.32	3.10	2.63	2.30	1.96	1.57
			REWMA	0.1231	0.6842	125.03	28.39	12.69	7.88	5.03	3.73	3.21	2.82	2.41	2.03
		1	TEWMA	0.3385	1.6123	164.81	43.10	16.20	8.18	4.20	2.76	2.26	1.92	1.57	1.22
			REWMA	0.4296	1.4864	177.37	49.58	18.60	9.19	4.61	3.01	2.45	2.08	1.71	1.32
	7	0.5	TEWMA	0.0980	0.6350	97.77	20.46	9.19	5.63	3.52	2.59	2.23	1.98	1.70	1.31
			REWMA	0.1628	0.8121	113.69	23.03	9.92	6.10	3.89	2.91	2.51	2.24	1.97	1.62
		1	TEWMA	0.3581	1.6838	146.27	32.91	11.79	5.99	3.19	2.17	1.80	1.55	1.28	1.06
			REWMA	0.3947	1.4069	151.38	34.69	12.43	6.37	3.47	2.40	2.02	1.74	1.45	1.13
	9	0.5	TEWMA	0.0938	0.6144	83.64	16.67	7.64	4.77	3.04	2.29	1.99	1.78	1.50	1.14
			REWMA	0.0835	0.5378	82.34	17.31	8.76	5.87	3.99	3.07	2.67	2.37	2.09	1.87
		1	TEWMA	0.3797	1.7621	133.29	26.83	9.35	4.80	2.63	1.83	1.53	1.32	1.13	1.01
			REWMA	0.5377	1.7275	153.30	34.47	11.63	5.60	2.88	1.93	1.60	1.37	1.15	1.02
6	3	0.5	TEWMA	0.1063	0.6751	117.54	26.65	11.70	7.00	4.25	3.05	2.59	2.27	1.94	1.55
			REWMA	0.1435	0.7517	128.17	28.84	12.51	7.62	4.80	3.54	3.04	2.67	2.29	1.94
		1	TEWMA	0.2289	1.1981	145.15	34.40	13.38	7.23	4.03	2.77	2.31	2.00	1.66	1.29
			REWMA	0.2753	1.1213	153.53	37.24	14.33	7.76	4.40	3.09	2.61	2.27	1.93	1.53
	5	0.5	TEWMA	0.2366	1.2282	114.88	21.93	8.40	4.72	2.79	2.02	1.71	1.49	1.24	1.04
			REWMA	0.3414	1.2827	131.09	26.12	9.51	5.18	3.03	2.19	1.87	1.63	1.35	1.08
		1	TEWMA	0.3212	1.5486	128.15	25.46	9.16	4.85	2.73	1.92	1.62	1.40	1.18	1.02
			REWMA	0.4823	1.6046	149.72	33.06	11.34	5.61	2.98	2.04	1.69	1.45	1.21	1.03
	7	0.5	TEWMA	0.1625	0.9273	82.91	14.31	6.09	3.72	2.38	1.79	1.54	1.33	1.12	1.01
			REWMA	0.2064	0.9392	90.44	15.35	6.61	4.15	2.72	2.11	1.86	1.66	1.36	1.06
		1	TEWMA	0.4719	2.0928	126.89	23.36	7.70	3.87	2.12	1.48	1.26	1.12	1.03	1.00
			REWMA	0.6003	1.8660	142.04	28.59	9.18	4.39	2.29	1.56	1.30	1.15	1.04	1.00
	9	0.5	TEWMA	0.0968	0.6293	59.62	10.97	5.20	3.36	2.26	1.76	1.52	1.30	1.09	1.00
			REWMA	0.2946	1.1695	89.03	13.66	5.48	3.35	2.19	1.68	1.43	1.23	1.06	1.00
		1	TEWMA	0.5793	2.4770	123.46	21.26	6.63	3.24	1.76	1.25	1.10	1.03	1.00	1.00
			REWMA	0.6375	1.9484	129.94	23.29	7.23	3.50	1.87	1.31	1.14	1.05	1.01	1.00

Table 5: The ARL_{min} comparisons between the upper-sided TEWMA $\bar{X}$ chart and the upper-sided REWMA $\bar{X}$ chart in the absence of measurement errors.

m	n	Scheme	Control Limits	δ_{opt}								
				0.1	0.25	0.5	0.75	1	1.5	2	2.5	3
1	3	TEWMA	λ_*	0.0462	0.0454	0.0950	0.1350	0.2879	0.4172	0.4280	0.4060	0.4211
			H_*^+	0.3568	0.3518	0.6207	0.8074	1.4244	1.8972	1.9360	1.8570	1.9113
			ARL_{min}	**90.1454**	**27.6980**	**10.3338**	**5.5871**	**3.5766**	**1.9592**	**1.3600**	**1.1044**	**1.0159**
		REWMA	λ_*	0.1250	0.0916	0.1554	0.2919	0.3421	0.6321	0.6156	0.4615	0.5067
			h_*^+	0.6907	0.5698	0.7896	1.1627	1.2843	1.9365	1.8999	1.5581	1.6589
			ARL_{min}	**114.5886**	**30.9037**	**11.1583**	**6.1065**	**3.9033**	**2.0801**	**1.3912**	**1.1710**	**1.0272**
	5	TEWMA	λ_*	0.1013	0.0903	0.1463	0.2407	0.3978	0.3985	0.4071	0.4375	0.3340
			H_*^+	0.6513	0.5971	0.8574	1.2442	1.8276	1.8301	1.8608	1.9699	1.5955
			ARL_{min}	**80.1199**	**20.3781**	**7.0200**	**3.7576**	**2.4305**	**1.4277**	**1.0803**	**1.0052**	**1.0002**
		REWMA	λ_*	0.1166	0.1047	0.2258	0.2996	0.5865	0.5977	0.5943	0.5166	0.6394
			h_*^+	0.6619	0.6193	0.9923	1.1819	1.8354	1.8602	1.8526	1.6808	1.9527
			ARL_{min}	**84.2254**	**21.2928**	**7.6289**	**4.1105**	**2.6536**	**1.4578**	**1.0883**	**1.0097**	**1.0001**
	7	TEWMA	λ_*	0.1033	0.0162	0.1806	0.3252	0.4357	0.3791	0.3915	0.4122	0.3865
			H_*^+	0.6606	0.1477	1.0034	1.5636	1.9634	1.7600	1.8047	1.8792	1.7866
			ARL_{min}	**64.7983**	**15.6131**	**5.4119**	**2.9099**	**1.9040**	**1.1991**	**1.0138**	**1.0002**	**1.0000**
		REWMA	λ_*	0.1036	0.1576	0.3528	0.4141	0.6067	0.6048	0.6233	0.6600	0.5384
			h_*^+	0.6151	0.7961	1.3096	1.4513	1.8801	1.8760	1.9169	1.9984	1.7290
			ARL_{min}	**65.4351**	**17.2928**	**6.0876**	**3.1737**	**2.0250**	**1.1992**	**1.0133**	**1.0002**	**1.0000**
	9	TEWMA	λ_*	0.1439	0.0690	0.1850	0.4014	0.4062	0.4251	0.4133	0.4251	0.3909
			H_*^+	0.8469	0.4868	1.0215	1.8404	1.8576	1.9254	1.8831	1.9253	1.8028
			ARL_{min}	**60.5551**	**12.7962**	**4.4667**	**2.4086**	**1.6283**	**1.0732**	**1.0016**	**1.0000**	**1.0000**
		REWMA	λ_*	0.2142	0.2916	0.3105	0.5256	0.6470	0.5932	0.6458	0.5888	0.6443
			h_*^+	0.9607	1.1620	1.2086	1.7005	1.9696	1.8503	1.9669	1.8405	1.9635
			ARL_{min}	**70.1897**	**16.6650**	**4.8652**	**2.6126**	**1.6699**	**1.0841**	**1.0016**	**1.0000**	**1.0000**
6	3	TEWMA	λ_*	0.0462	0.0428	0.1133	0.1882	0.2469	0.3351	0.3811	0.3969	0.3709
			H_*^+	0.3568	0.3359	0.7080	1.0345	1.2681	1.5999	1.7670	1.8242	1.7303
			ARL_{min}	**90.1454**	**27.5792**	**10.3964**	**5.5727**	**3.5774**	**2.0030**	**1.3841**	**1.1065**	**1.0191**
		REWMA	λ_*	0.1830	0.2041	0.1434	0.2155	0.3330	0.6412	0.4736	0.6226	0.6083
			h_*^+	0.8724	0.9326	0.7516	0.9643	1.2628	1.9566	1.5852	1.9153	1.8837
			ARL_{min}	**127.2120**	**38.8986**	**11.1147**	**6.0502**	**3.9058**	**2.0796**	**1.4906**	**1.1062**	**1.0178**
	5	TEWMA	λ_*	0.0301	0.1062	0.1255	0.2548	0.3931	0.4010	0.3772	0.4310	0.4281
			H_*^+	0.2527	0.6747	0.7644	1.2986	1.8105	1.8390	1.7530	1.9467	1.9364
			ARL_{min}	**62.6425**	**20.9048**	**7.0034**	**3.7562**	**2.4304**	**1.4254**	**1.0871**	**1.0053**	**1.0001**
		REWMA	λ_*	0.0735	0.1019	0.1583	0.3071	0.5060	0.5851	0.6190	0.5371	0.6588
			h_*^+	0.4966	0.6090	0.7986	1.2002	1.6572	1.8322	1.9074	1.7262	1.9958
			ARL_{min}	**75.1245**	**21.2275**	**7.6193**	**4.1060**	**2.6387**	**1.4648**	**1.0827**	**1.0087**	**1.0001**
	7	TEWMA	λ_*	0.0664	0.1495	0.2171	0.3420	0.4128	0.4281	0.3959	0.3883	0.3575
			H_*^+	0.4725	0.8715	1.1515	1.6251	1.8815	1.9361	1.8208	1.7932	1.6817
			ARL_{min}	**58.0558**	**16.8974**	**5.4388**	**2.9087**	**1.9126**	**1.1799**	**1.0136**	**1.0002**	**1.0000**
		REWMA	λ_*	0.1615	0.1991	0.2486	0.4344	0.6321	0.5939	0.6178	0.5102	0.4757
			h_*^+	0.8082	0.9187	1.0527	1.4973	1.9364	1.8518	1.9047	1.6665	1.5898
			ARL_{min}	**75.0261**	**18.3184**	**5.8797**	**3.1727**	**2.0210**	**1.2036**	**1.0136**	**1.0004**	**1.0000**
	9	TEWMA	λ_*	0.0602	0.2059	0.2280	0.3854	0.4373	0.4307	0.4271	0.4254	0.4422
			H_*^+	0.4383	1.1066	1.1944	1.7828	1.9691	1.9457	1.9326	1.9266	1.9867
			ARL_{min}	**47.9762**	**14.6630**	**4.4626**	**2.4112**	**1.6138**	**1.0722**	**1.0015**	**1.0000**	**1.0000**
		REWMA	λ_*	0.1227	0.0557	0.3458	0.5314	0.5480	0.6055	0.6170	0.4832	0.5463
			h_*^+	0.6828	0.4162	1.2931	1.7135	1.7502	1.8775	1.9029	1.6065	1.7465
			ARL_{min}	**57.6001**	**14.2727**	**4.8973**	**2.6133**	**1.7182**	**1.0813**	**1.0018**	**1.0000**	**1.0000**

Table 6: The ARL_{min} comparisons between the upper-sided TEWMA $\bar{X}$ chart and the upper-sided REWMA $\bar{X}$ chart in the presence of measurement errors.

m	n	Scheme	Control Limits	δ_{opt}								
				0.1	0.25	0.5	0.75	1	1.5	2	2.5	3
1	3	TEWMA	λ_*	0.0716	0.1590	0.1792	0.2062	0.1028	0.2677	0.5004	0.6581	0.8353
			H_*^+	0.5011	0.9121	0.9976	1.1077	0.6585	1.3482	2.1944	2.7625	3.4272
			ARL_{min}	**138.3041**	**60.8934**	**20.3150**	**10.1285**	**6.1795**	**3.2739**	**2.1213**	**1.5275**	**1.2149**
		REWMA	λ_*	0.2733	0.1236	0.1483	0.1431	0.1617	0.3962	0.5819	0.6571	0.4593
			h_*^+	1.1162	0.6860	0.7673	0.7506	0.8088	1.4104	1.8253	1.9920	1.5530
			ARL_{min}	**186.8310**	**56.0892**	**19.4518**	**10.1708**	**6.6898**	**3.5695**	**2.2859**	**1.6185**	**1.4032**
	5	TEWMA	λ_*	0.1438	0.0936	0.1066	0.1902	0.3385	0.4731	0.6166	0.8702	0.8735
			H_*^+	0.8464	0.6137	0.6766	1.0429	1.6123	2.0972	2.6115	3.5627	3.5754
			ARL_{min}	**129.0396**	**35.2880**	**11.9614**	**6.4592**	**4.2038**	**2.2269**	**1.4640**	**1.1328**	**1.0256**
		REWMA	λ_*	0.3703	0.1266	0.1231	0.2318	0.4296	0.5466	0.6388	0.6529	0.6487
			h_*^+	1.3506	0.6963	0.6842	1.0085	1.4864	1.7471	1.9513	1.9826	1.9732
			ARL_{min}	**169.5184**	**38.3267**	**12.6903**	**6.9586**	**4.6145**	**2.4062**	**1.5542**	**1.1868**	**1.0445**
	7	TEWMA	λ_*	0.1113	0.0661	0.0980	0.2457	0.3581	0.5441	0.7921	0.8222	0.8853
			H_*^+	0.6985	0.4709	0.6350	1.2635	1.6838	2.3508	3.2618	3.3766	3.6219
			ARL_{min}	**101.2541**	**25.6774**	**9.1899**	**4.9791**	**3.1931**	**1.7340**	**1.1919**	**1.0304**	**1.0024**
		REWMA	λ_*	0.0403	0.2043	0.1628	0.3254	0.3947	0.5999	0.5272	0.5898	0.6330
			h_*^+	0.3375	0.9333	0.8121	1.2446	1.4069	1.8650	1.7041	1.8427	1.9383
			ARL_{min}	**84.1534**	**34.1450**	**9.9182**	**5.4368**	**3.4708**	**1.8567**	**1.3194**	**1.0603**	**1.0054**
	9	TEWMA	λ_*	0.0939	0.1063	0.0938	0.3164	0.3797	0.7082	0.9300	0.9197	0.9326
			H_*^+	0.6149	0.6750	0.6144	1.5309	1.7621	2.9470	3.7988	3.7577	3.8090
			ARL_{min}	**83.6528**	**22.7692**	**7.6396**	**4.1257**	**2.6322**	**1.4490**	**1.0765**	**1.0059**	**1.0002**
		REWMA	λ_*	0.0393	0.1049	0.0835	0.2976	0.5377	0.6487	0.6019	0.6173	0.5720
			h_*^+	0.3320	0.6198	0.5378	1.1770	1.7275	1.9732	1.8695	1.9037	1.8033
			ARL_{min}	**72.5934**	**23.0900**	**8.7593**	**4.4437**	**2.8766**	**1.5371**	**1.1297**	**1.0132**	**1.0007**
6	3	TEWMA	λ_*	0.0135	0.0591	0.1063	0.2772	0.2289	0.4492	0.7361	0.8282	0.8875
			H_*^+	0.1248	0.4320	0.6751	1.3843	1.1981	2.0118	3.0507	3.3998	3.6306
			ARL_{min}	**81.8784**	**31.7378**	**11.7016**	**6.6045**	**4.0253**	**2.1798**	**1.4350**	**1.1200**	**1.0218**
		REWMA	λ_*	0.0507	0.0760	0.1435	0.2140	0.2753	0.5600	0.4982	0.5622	0.6586
			h_*^+	0.3919	0.5070	0.7517	0.9602	1.1213	1.7768	1.6398	1.7817	1.9955
			ARL_{min}	**102.7650**	**33.7205**	**12.5081**	**6.7924**	**4.4039**	**2.3532**	**1.6136**	**1.2055**	**1.0375**
	5	TEWMA	λ_*	0.0716	0.0857	0.2366	0.1990	0.3212	0.7127	0.8587	0.9159	0.9826
			H_*^+	0.5011	0.5739	1.2282	1.0788	1.5486	2.9636	3.5176	3.7424	4.0106
			ARL_{min}	**80.6521**	**22.8235**	**8.4013**	**4.2385**	**2.7346**	**1.5004**	**1.0934**	**1.0084**	**1.0003**
		REWMA	λ_*	0.2480	0.0747	0.3414	0.3493	0.4823	0.5305	0.5307	0.4404	0.5907
			h_*^+	1.0512	0.5018	1.2827	1.3014	1.6046	1.7116	1.7120	1.5107	1.8448
			ARL_{min}	**116.9214**	**23.2366**	**9.5090**	**4.6333**	**2.9750**	**1.6544**	**1.1830**	**1.0403**	**1.0010**
	7	TEWMA	λ_*	0.0241	0.0411	0.1625	0.3081	0.4719	0.7929	0.9336	0.7232	0.8469
			H_*^+	0.2097	0.3253	0.9273	1.5002	2.0928	3.2646	3.8130	3.0025	3.4721
			ARL_{min}	**54.8394**	**17.0811**	**6.0902**	**3.2715**	**2.1190**	**1.2144**	**1.0174**	**1.0005**	**1.0000**
		REWMA	λ_*	0.0605	0.0764	0.2064	0.4017	0.6003	0.6508	0.6563	0.6433	0.6251
			h_*^+	0.4391	0.5089	0.9392	1.4229	1.8660	1.9780	1.9902	1.9613	1.9208
			ARL_{min}	**64.5338**	**18.2950**	**6.6096**	**3.5702**	**2.2858**	**1.2826**	**1.0310**	**1.0010**	**1.0000**
	9	TEWMA	λ_*	0.0716	0.0987	0.0968	0.4221	0.5793	0.8873	0.8757	0.8996	0.9473
			H_*^+	0.5011	0.6386	0.6293	1.9147	2.4770	3.6295	3.5843	3.6782	3.8680
			ARL_{min}	**55.3801**	**14.6096**	**5.2029**	**2.7141**	**1.7579**	**1.0888**	**1.0028**	**1.0000**	**1.0000**
		REWMA	λ_*	0.1207	0.0721	0.2946	0.4424	0.6375	0.5572	0.6493	0.6395	0.6271
			h_*^+	0.6760	0.4905	1.1695	1.5153	1.9484	1.7706	1.9746	1.9528	1.9252
			ARL_{min}	**63.9414**	**15.4095**	**5.4832**	**2.9462**	**1.8741**	**1.1639**	**1.0060**	**1.0000**	**1.0000**

Table 7: A real example for detecting the downward mean shift of the yogurt cup filling process.

t	$Y_{t,1}$		$Y_{t,2}$		$Y_{t,3}$		$Y_{t,4}$		$Y_{t,5}$		$\bar{Y}_t$	W_t^-	Q_t^-
	$Y_{t,1,1}$	$Y_{t,1,2}$	$Y_{t,2,1}$	$Y_{t,2,2}$	$Y_{t,3,1}$	$Y_{t,3,2}$	$Y_{t,4,1}$	$Y_{t,4,2}$	$Y_{t,5,1}$	$Y_{t,5,2}$			
1	124.78	125.33	124.19	124.22	124.55	124.22	123.98	124.25	124.97	125.42	124.59	-0.1654	-0.1551
2	124.54	124.51	124.39	124.85	125.00	124.91	124.82	124.73	123.81	123.20	124.48	-0.4100	-0.3408
3	124.25	124.33	124.48	124.42	123.10	123.80	125.74	125.59	123.34	123.45	124.25	-0.8261	-0.6075
4	125.25	125.62	124.78	124.52	124.52	124.58	125.42	125.31	124.89	124.77	124.97	-0.5275	-0.4682
5	124.44	124.55	124.74	124.33	125.93	126.20	125.43	125.56	125.71	125.22	125.21	-0.2881	-0.2302
6	125.39	124.87	125.46	125.26	125.67	125.43	125.00	125.45	125.13	125.61	125.33	-0.0959	0
7	124.98	124.38	125.06	124.60	125.63	125.77	124.42	124.22	124.85	124.69	124.86	0.0193	-0.0201
8	124.17	124.88	126.13	125.77	125.50	124.68	125.21	125.72	125.37	124.92	125.24	0.1506	0
9	125.62	125.58	125.95	125.21	125.25	125.07	124.14	124.17	125.06	124.92	125.10	0.2560	0
10	127.00	127.15	124.77	124.88	125.32	124.93	125.18	125.70	123.47	123.85	125.23	0.3405	0
11	124.30	123.85	125.41	124.47	124.41	124.53	124.12	124.20	124.87	125.08	124.52	0.0425	-0.1887
12	125.16	125.18	123.80	123.91	124.57	124.12	124.40	124.57	123.58	123.62	124.29	-0.4231	-0.4614
13	125.18	124.86	125.47	125.06	125.47	125.50	125.02	125.23	125.61	125.59	125.30	-0.2043	-0.1805
14	125.20	124.68	123.16	123.07	124.76	124.73	123.58	123.45	123.51	123.41	123.96	-0.9480	-0.6233
15	123.72	123.53	125.22	124.82	124.77	124.37	125.08	125.00	124.48	124.11	124.51	**-1.0047**	-0.7101
16	123.73	123.81	127.45	126.98	124.32	123.39	124.19	124.79	123.87	124.22	124.68	-0.8897	-0.6989
17	124.00	123.55	125.12	125.00	126.51	126.42	124.41	124.83	124.66	123.97	124.85	-0.6302	-0.6033
18	123.47	123.79	124.53	124.87	124.18	124.30	125.05	124.74	124.54	124.37	124.38	-0.8723	-0.7569
19	124.47	124.52	124.47	124.08	122.82	123.28	124.94	125.04	124.37	124.50	124.25	-1.1979	**-0.9513**
20	123.86	124.07	125.48	125.37	125.76	125.89	125.67	125.62	125.69	125.78	125.32	-0.8259	-0.5747

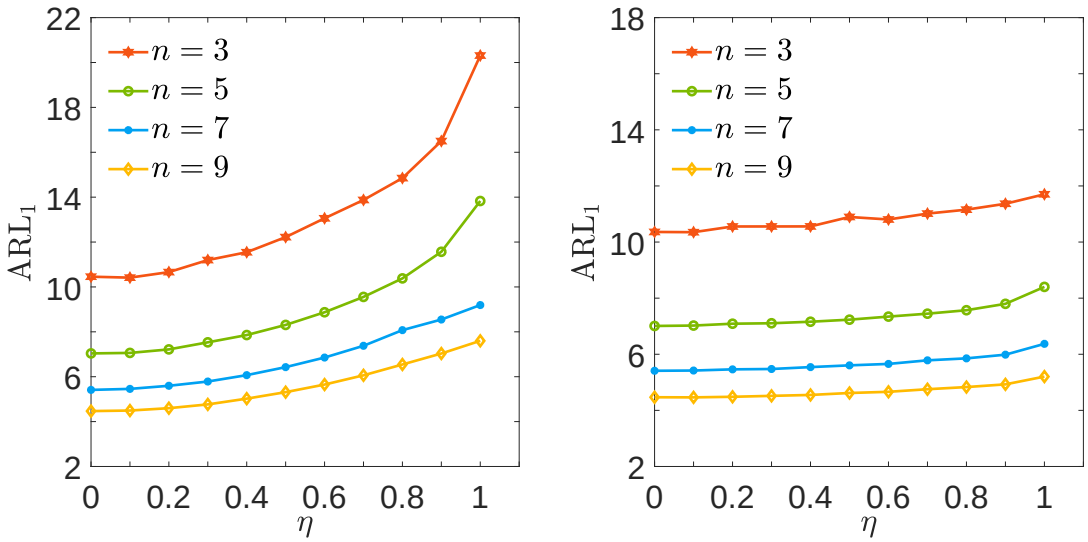

Figure 1: The effect of η on the overall performance of the upper-sided TEWMA $\bar{X}$ scheme with measurement errors for $n \in \{3, 5, 7, 9\}$ when $A = 0$, $B = 1$, $\delta_{opt} = 0.5$, $m \in \{1, 6\}$, and $\text{ARL}_0 = 370$.

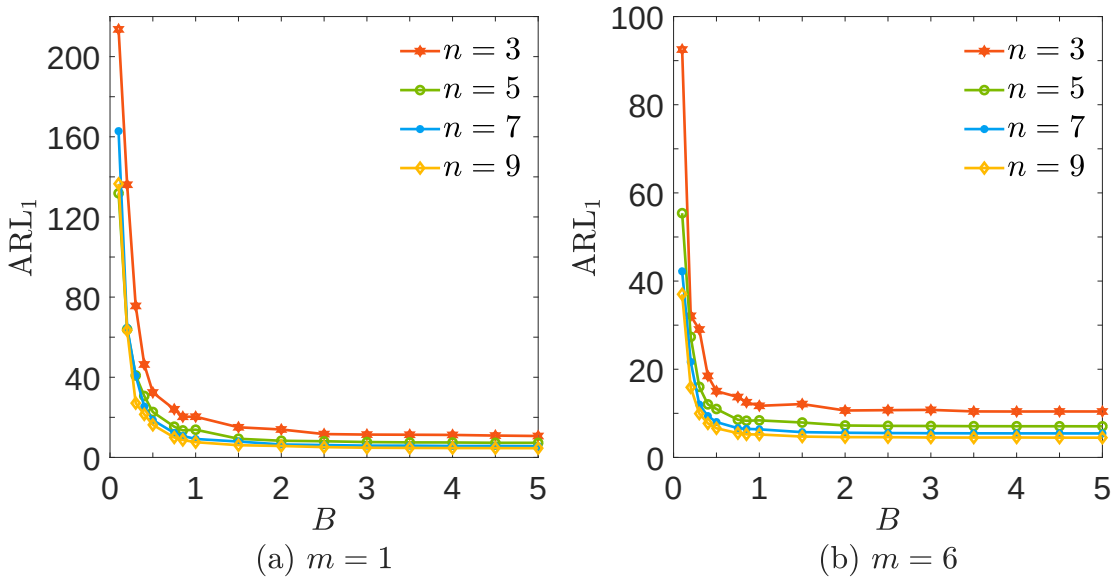

(a) $m = 1$ (b) $m = 6$

Figure 2: The effect of B on the overall performance of the upper-sided TEWMA $\bar{X}$ scheme with measurement errors for $n \in \{3, 5, 7, 9\}$ when $A = 0$, $\eta = 1$, $\delta_{opt} = 0.5$, $m \in \{1, 6\}$, and $\mathrm{ARL}_0 = 370$.

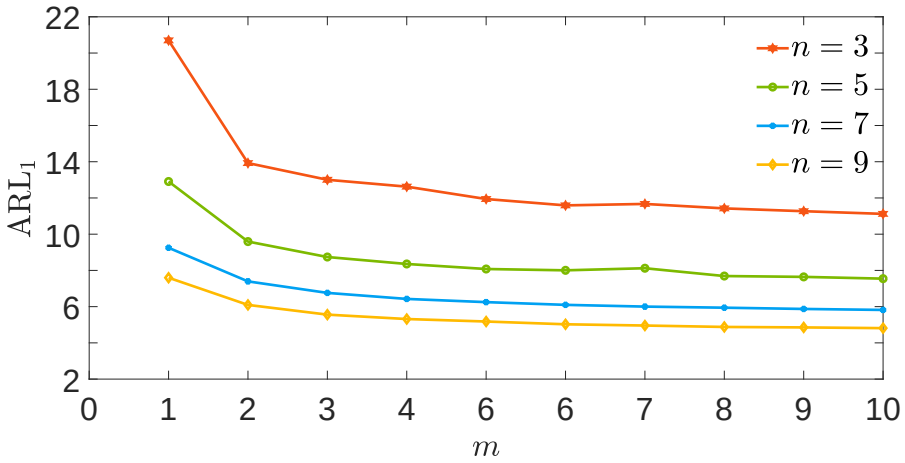

Figure 3: The effect of m on the overall performance of the upper-sided TEWMA $\bar{X}$ scheme with measurement errors for $n \in \{3, 5, 7, 9\}$ when $A = 0$, $B = 1$, $\eta = 1$, $\delta_{opt} = 0.5$, and $\mathrm{ARL}_0 = 370$.

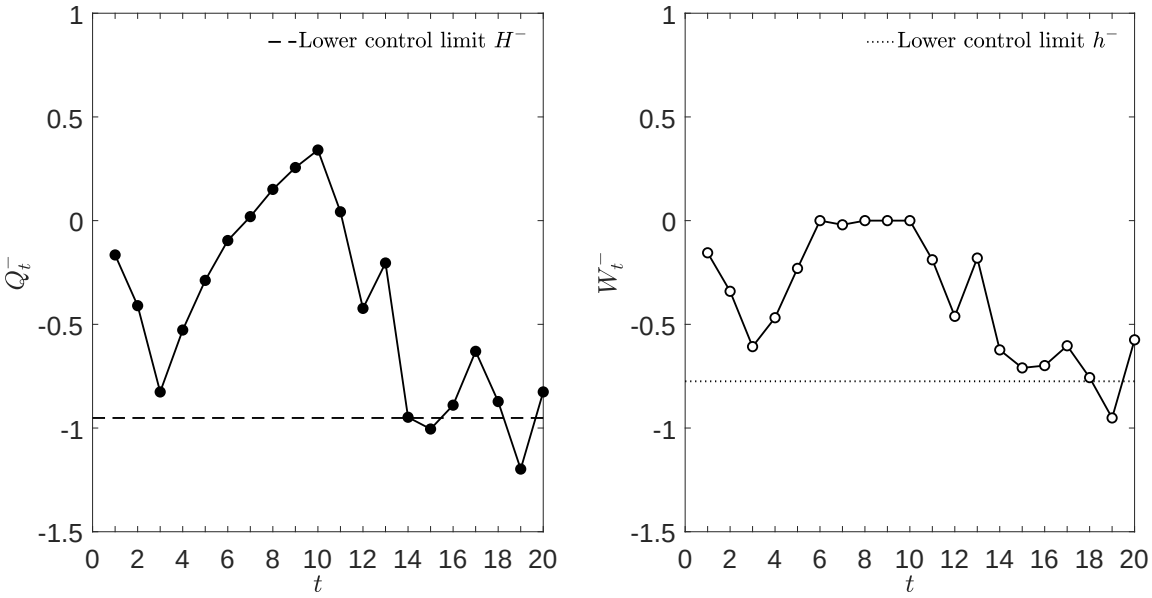

(a) Lower-sided TEWMA $\bar{X}$ chart (b) Lower-sided REWMA $\bar{X}$ chart

Figure 4: The monitoring procedure of the lower-sided TEWMA $\bar{X}$ and lower-sided REWMA $\bar{X}$ schemes for detecting the downward mean shift of the yogurt cup filling process.